Available online at www.sciencedirect.com

ScienceDirect

journal homepage: www.elsevier.com/locate/he

Review Article

A short review on generation of green fuel hydrogen through water splitting

*Poulami Hota, Aranya Das, Dilip K. Maiti**

Department of Chemistry, University of Calcutta, 92, A. P. C. Road, Kolkata, 700009, India

HIGHLIGHTS

- Light or electricity driven water-splitting produces green hydrogen.
- Electrocatalytic hydrogen evolution requires efficient low cost electrocatalyst.
- Metal chalcogenides, oxides, low pt content materials act as good electrocatalyst.
- Different semiconductor photocatalysts are used in photocatalytic H_2 generation.
- Mechanism of photo and electrocatalytic hydrogen production are discussed.

GRAPHICAL ABSTRACT

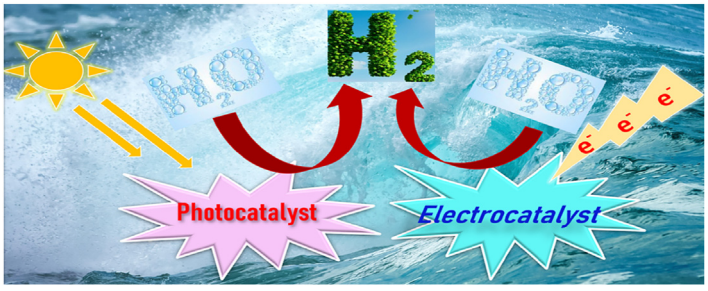

ARTICLE INFO

Article history:
Received 5 July 2022
Received in revised form
16 September 2022
Accepted 27 September 2022
Available online 20 October 2022

Keywords:
Green fuel hydrogen
Water splitting
Photocatalytic hydrogen evolution
Earth abundant photocatalyst
Electrocatalytic hydrogen evolution
Low cost electrocatalyst

ABSTRACT

Hydrogen is considered as a promising clean and renewable energy carrier and an attractive alternative to fossil fuels. A potential and cheapest way to produce hydrogen is involving water splitting either by light or electricity. The vital step involved in water splitting is the hydrogen evolution reaction (HER) which requires the use of an efficient catalyst to lower its large overpotential value. Therefore, the development of earth-abundant photocatalysts and electrocatalysts with high activity and long-term stability for hydrogen generation gains major attention. The present review summarizes the mechanism of hydrogen production via water splitting utilizing different metal-based and metal-free photocatalysts and electrocatalysts. Different strategies adopted to improve the catalytic activity of electrocatalysts and photocatalysts for water splitting are discussed. Finally, the challenges and future scope of hydrogen evolution reaction are briefly summarized.

* *Corresponding author.*
E-mail address: dkmchem@caluniv.ac.in (D.K. Maiti).

https://doi.org/10.1016/j.ijhydene.2022.09.264

Contents

Introduction

Today our visionary ideas will decide the quality of life for our future generation. The development of modern society needs the maximum use of fossil fuel which produces harmful greenhouse gas such as carbon dioxide (CO_2), carbon monoxide (CO), etc. in the environment. These harmful gases have diverse effects on the health of living organisms and affect the global climate severely. The gases absorb sunlight and solar radiation that have bounced off the earth's surface, thereby increasing the temperature of the earth's atmosphere, termed global warming. This global climate scenario, coupled with the shortage of fossil fuels and rapid increase in energy consumption, encourages the finding of alternative sustainable and renewable energy sources. Therefore, in such a critical situation, renewable and clean alternative development is needed so that a beautiful pollution-free environment can be provided for future generations. Highest gravimetric energy density and environmental friendliness (combustion by product is pollution-free water) make molecular hydrogen (H_2) an excellent energy carrier. Recent production of hydrogen (90%) mainly involves steam reforming process which requires fossil fuels for conversion and emits CO_2. Therefore, a clean, renewable and effective hydrogen production route is necessary for sustainable development of hydrogen economy. Different renewable energy-based hydrogen production methods are available (Fig. 1) [1]. Among them, water splitting either by light or electricity has been considered a potential hydrogen generation method [2–5]. Electrocatalytic hydrogen production needs electricity obtained from renewable sources (wind, water, or sun) whereas photocatalytic hydrogen generation directly utilizes solar energy and thus can effectively reduce the overall energy consumption for the hydrogen generation process. Therefore, photocatalytic hydrogen generation appears to be a much clean and renewable hydrogen generation method in comparison to electrocatalytic hydrogen evolution although both processes produce green fuel hydrogen [6]. Both processes require an efficient catalyst which will lower the activation energy of the process, making the process more feasible. Different noble metal-based catalysts such as platinum, iridium, ruthenium and their alloys show good catalytic activity towards electrocatalytic and photocatalytic hydrogen generation due to their appropriate band gap and optimum hydrogen binding energies. However, high cost and low natural abundance limit their practical applications. Therefore, exploration of less expensive, earth abundant photocatalysts and electrocatalysts is necessary for the industrial production of hydrogen through water splitting. Different transition metal oxides and sulphides have been

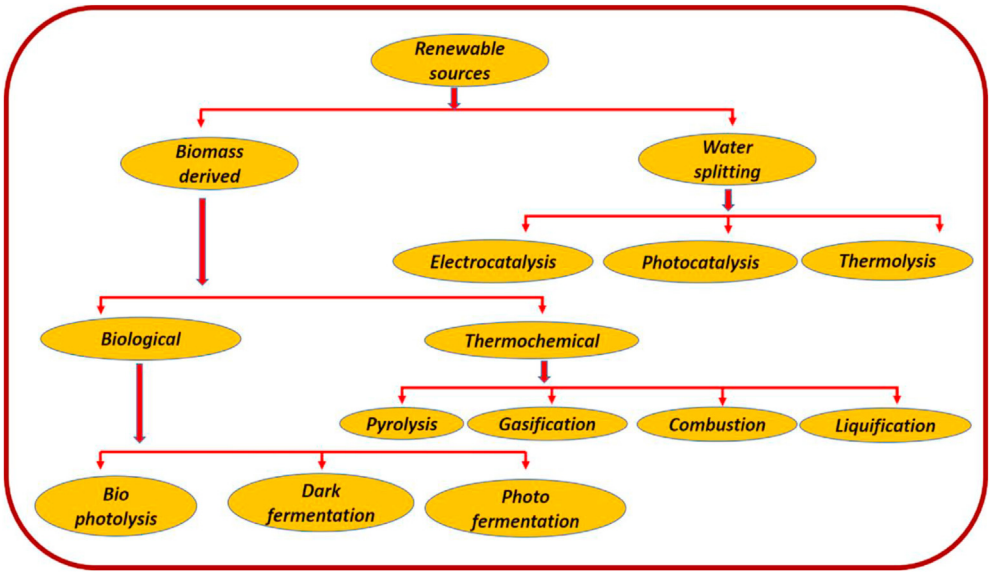

Fig. 1 – Hydrogen production techniques based on renewable energy sources.

thoroughly investigated for their electrocatalytic activity and photocatalytic activity [7–9]. Hydrogen evolution photocatalyst must obey certain basic criteria such as the photocatalyst should have appropriate band position and band energy and must be capable of absorbing light energy and thus generating electro-hole pairs which facilitate hydrogen generation at a reasonably faster rate. Earlier (1972) Fujishima and Honda utilize titanium dioxide as an efficient photocatalyst for hydrogen generation under ultra-violet radiation [10]. However, TiO_2 fails to work under visible light since its light absorption activity is limited in the ultraviolet region which reduces its photocatalytic efficiency. Hence, several techniques have been used for band gap engineering of TiO_2 such as doping of metals and nonmetals, coupling with suitable semiconductors and synthesizing ternary metal structure. Apart from this metal-based photocatalysts, graphitic carbon nitride (g-C_3N_4) based catalysts are largely studied as metal-free semiconductor photocatalyst due to their narrow band gap (2.7 eV) visible light responsive behaviour [11]. Quantum dot based photocatalysts such as cadmium-based and cadmium-free photocatalysts are also widely studied as hydrogen evolution photocatalyst [12]. Apart from the field of photocatalysts, substantial research has been carried out on the development of electrocatalysts. Electrocatalysts use electricity for water splitting and they must have appropriate hydrogen binding energies and gives free energy for the hydrogen adsorption-desorption process. In search of less expensive electrocatalysts, low noble metal content catalysts, different transition metal (Molybdenum, Tungsten and others) chalcogenides, oxides, carbides and nitrides are thoroughly investigated [13,14]. However, most of them suffer from conductivity and stability related issues. Therefore, in recent times scientists focused on metal-free electrocatalysts which will overcome these challenges. The present review mainly discusses the generation of hydrogen fuel via water splitting utilizing different nanostructures as electrocatalysts and photocatalysts, and the mechanism of hydrogen production has been discussed elaborately.

Photocatalytic hydrogen production

Photocatalytic hydrogen evolution via water splitting is a potential approach for producing green hydrogen due to its low cost, low energy consumption, and environmental friendliness. The semiconductor photocatalyst that harnesses solar energy for water splitting is the basis for photocatalytic hydrogen evolution. Irradiation of light of suitable wavelength (Photon of particular energy) excites valence band electron of photocatalyst into the conduction band (CB), thereby generating the electron (e^-)–hole (h^+) pairs, responsible for redox reaction occurring on photocatalysts' surface. Basic concepts of photocatalytic hydrogen evolution and mechanistic studies of various photocatalysts are discussed in the following section (Fig. 2).

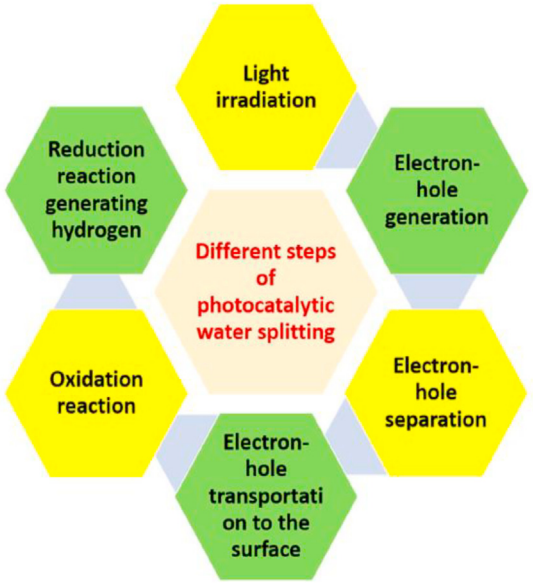

Fig. 2 – Important steps involved in the photocatalytic water splitting reaction.

Fundamentals of photocatalytic hydrogen evolution

Photocatalysis is defined as a change in the rate of a chemical reaction in the presence of light (ultraviolet/visible/IR) using a suitable photocatalyst that facilitates the chemical reaction by absorbing light. The reactions which satisfy the conditions are termed photocatalytic reactions. These reactions involve several significant steps. The primary initiation step is light harvesting in which the photocatalyst is activated with a photon (light quanta) of suitable energy. The next step is charge excitation, where electrons from the valence band (VB) of semiconductor photocatalyst are excited to the conduction band (CB) generating photoexcited hole in the valence band and photoexcited electron in the conduction band of photocatalyst. These photo-excited holes and electrons are powerful oxidants and reductants causing redox reactions. However, the major problem of photocatalytic water splitting is the recombination of photogenerated electron-hole pairs. To obtain equilibrium, photoexcited electrons in the CB fall back to VB via radiative or nonradiative transition causing recombination, which destroys free electron–hole pairs. Survived free electron–hole pairs are transported to the active site of the catalyst surface via diffusion or due to the electric field generated from photocatalyst/electrolyte and photocatalyst/cocatalyst interfaces. These transported photoexcited holes cause oxidation of water, producing protons (H^+), whereas transported photoexcited electrons are involved in the reduction of H^+ producing molecular hydrogen. In a photocatalyst, the conduction band position must be lower in energy than the reduction potential of H^+/H_2 couple and the valence band maximum should be higher in energy than the oxidation potential of H_2O/O_2 couple [15].

In case of pure water, recombination phenomena occur at a faster rate. To improve process efficiency, photocatalytic water splitting is typically performed in the presence of suitable cocatalysts (alcohol, glycerol, etc.) and electrolytes (sodium sulphide, potassium iodide etc.). Cocatalysts or sacrificial agents are electron donors which interact with the VB holes stabilizing charge separation. Whereas electrolytes improve the conductivity of the solution, facilitating faster electron transfer to the semiconductor photocatalyst thereby increasing the efficiency of the process.

Thermodynamic aspects

Change in Gives free energy (ΔG) of the process is another important criterion for the photocatalytic reactions. In general, for a chemical reaction to be spontaneous ΔG should be negative. However, in case of photocatalytic reactions, a reaction may proceed even with positive ΔG because overall redox reaction is feasible under this condition. Photocatalytic water splitting reaction is a thermodynamically uphill reaction with Gives free energy change (ΔG) equal to 237 kJ mol^{-1}. Now Gives free energy change (ΔG) is related to the electrode potential (E^0) according to the following equation as $\Delta G = -nFE^0$ where n is number of electrons involved during the reaction, F is faraday constant. Calculating from this equation, the minimum potential required for photocatalytic water splitting is 1.23 eV. Therefore, semiconductors having a minimum band gap of 1.23 eV are eligible as photocatalysts. The minimum potential required for photocatalytic water splitting is calculated by considering 100% quantum efficiency and light absorbance efficiency of the photocatalyst which predicts 47.2% solar to hydrogen (STH) conversion efficiency. In practice, the interfacial charge transfer process is associated with overpotential and reorganisation energies, which raise the minimum potential requirement for the photocatalytic hydrogen evolution process and reduces the STH efficiency by nearly 18%. Therefore, a semiconductor photocatalyst having band gap of more than 1.23 eV is always recommended. The nature of radiation used for photocatalytic reactions depends on semiconductor bandgap. Generally, large bandgap semiconductors (>3.15 eV) are activated under UV light (wavelength 200–400 nm) irradiation, while narrow band gap semiconductors are activated by visible light (wavelength 400–800 nm). There are mainly two criteria for choosing a photocatalyst for a water splitting reaction. The primary condition is the band gap of the semiconductor photocatalyst must be within the range of 1.23 eV–3.26 eV. The secondary condition is the band positions of the photocatalyst, where CB minimum positions of the catalyst must be at a negative potential than the reduction potential of H^+/H_2 (−0.41 eV vs NHE at pH~7) and VB maximum position at a more positive potential than the O_2/H_2O (+0.82 eV vs NHE at pH ~7) [16]. These conditions discussed so far are applied to traditional photocatalysts. Jinlong Yang and his group theoretically predicted that two-dimensional (2D) material with a vertical intrinsic electric field (EF) breaks the conventional band gap limit (1.23 eV) of the photocatalysts and broadens the light absorption region. The group shows among different two-dimensional M_2X_3 (M = Al, Ga, In; X = S, Se, Te) structures In_2Te_3 is found to be IR driven photocatalyst with maximum STH efficiency (32.1%) [17]. Later Chuan-LuYang and his group theoretically studied the photocatalytic efficiency of two-dimensional TeX (X = C, Si, Ge) monolayers having a strong intrinsic electric field. TeC monolayer shows maximum STH efficiency, 32.74% under 8% biaxial strain [18].

Different photocatalyst systems

Photocatalytic hydrogen evolution may occur either by the half-cell reaction of water dissociation that only the reduction reaction of proton to molecular hydrogen or overall water splitting reaction involving both oxidation as well as reduction reaction.

Overall water splitting reaction:

$$2H_2O \rightarrow O_2 + 2H_2$$

Half-cell reduction reaction:

$$4H^+ + 4e^- \rightarrow 2H_2$$

Half-cell oxidation reaction:

$$2H_2O \rightarrow O_2 + 4H^+$$

Photocatalytic hydrogen generation via the half-cell reduction reaction is usually carried out in the presence of

sacrificial agents or reducing agents such as triethyl amine, alcohol etc. Photogenerated holes react with these sacrificial agents instead of water, producing electrons which increases the photocatalyst's hydrogen generation efficiency.

Over the years, various photocatalysts (PC) have been reported for photocatalytic hydrogen generation, which is generally categorized into single-photon (single-step) and two photon (two-step) systems (Fig. 3). Single component semiconductor photocatalyst should have compatible band gap and position with respect to the potential of H^+/H_2 and O_2/H_2O couple. In 1972 Fujishima and Honda first reported the use of titanium dioxide (TiO_2) as a photocatalyst. However wider band gap (3.2 eV) limits their application under visible light. Furthermore, the strong coulombic interaction between electron and hole results in the recombination of the photogenerated electron-hole pairs, resulting in low efficiency of a single component photocatalyst. Coupling titanium dioxide with a low band gap semiconductor such as graphitic carbon nitride (band gap 2.7 eV) reduces bandgap, causing faster charge separation, thereby increasing their photocatalytic activity. Thus g-C_3N_4/TiO_2 heterostructure composite shows excellent photocatalytic activity under visible light [19].

Heterojunction structures efficiently prevent recombination of photogenerated electron–hole pairs. In general, two different semiconductors having staggered band structures construct heterojunctions. When heterojunctions are exposed to solar light, both photocatalysts become excited, resulting in photogenerated electron-hole pairs in which electrons from the higher conduction band (CB) position of PC-I migrate to the lower CB position of PC-II and the photogenerated holes migrate in reverse. Finally, the photoinduced electron-hole pairs generated on PC- II effect reduction reaction and electron-hole pairs generated on PC-I cause the oxidation reaction (Fig. 3(b)). This promotes spatial separation and prevents the recombination of charge carriers [20].

Another important class of photocatalyst is Z-scheme charge carrier based photocatalyst systems, made of two types of photocatalyst. One is an oxidation photocatalyst with strong oxidising property and a lower energy valence band position (involved in oxygen evolution), and the other is a reduction photocatalyst with a strong reducing property and a higher conduction band position (involve in hydrogen evolution). In this case, the reduction abilities of photogenerated electrons residing in the higher CB position of PC-I and oxidation properties of photogenerated holes remaining in the valence band (VB) of PC-II are retained and recombination occurs between photogenerated electrons in the CB of PC-II and holes in the VB of PC (Fig. 3(c)). This induces spatially differentiated active sites, which increases the catalytic activity of the photocatalyst.

Z-scheme photocatalysts are classified into three main categories: traditional Z-scheme photocatalysts, all solid-state Z-scheme photocatalysts and direct Z-scheme photocatalysts (see Fig. 4). Traditional Z-scheme photocatalysts consist of reversible redox couple (Fe^{3+}/Fe^{2+}, IO_3^-/I^-) as electron transportation chains between the coupled photocatalysts. In the case of all solid-state Z-scheme photocatalysts, solid conductors such as noble metal nanoparticles, graphene, carbon nanotubes are used as electron mediators. Back reaction occurs in case of ionic redox mediators can be avoided using these solid conductors. However, these are expansive and generate shielding effect. The concept of direct Z-scheme photocatalysts is relatively new. In this case, no charge transport mediator is used between photocatalysts, which eliminates the scope of backward reactions and shielding effect. They are also resistant to corrosion. In the next section, different examples of photocatalysts used so far will be discussed [20].

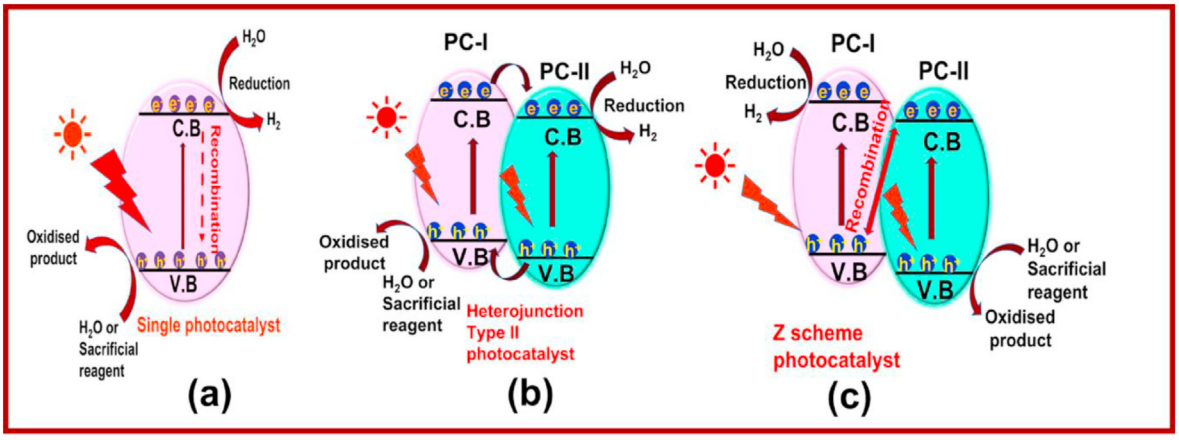

Fig. 3 – Schematic representation of different photocatalytic hydrogen generation systems via water splitting. (a) single step photocatalyst, (b) Type-II heterojunction photocatalyst, (c) direct Z-scheme photocatalyst.

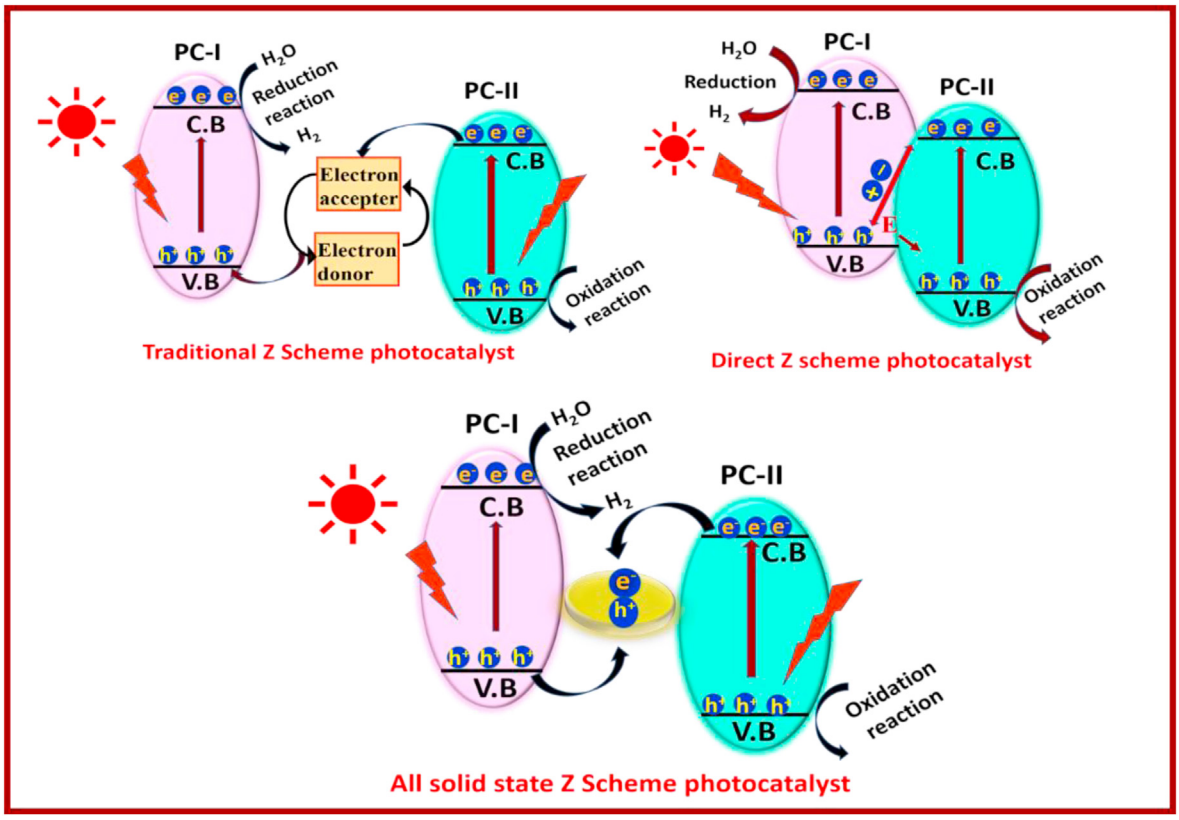

Fig. 4 – Schematic representation of different Z scheme photocatalytic hydrogen generation systems through water splitting.

Development in photocatalytic water splitting

Titania (TiO_2)-based photocatalysts

Titania-based photocatalysts are the most important for photocatalytic hydrogen evolution due to their low cost, non-toxicity, high stability, and high photocatalytic efficiency. There are three different phases of TiO_2 namely, the rutile phase, brookite phase and anatase phase. Among them, only the anatase phase has a suitable band gap (3.2 eV) and kinetic stability for photocatalytic water splitting reaction. However, TiO_2 is a wide bandgap (3.2 eV) semiconductor, activated by only ultra violet (UV) light limiting its activity in solar water splitting. Since the solar light spectrum lies mainly in the visible to infra-red region, and only 4% UV components are present in the solar spectrum. Therefore, several attempts have been made for band gap engineering of TiO_2 which include doping of metals and nonmetals, coupling with suitable semiconductors, synthesizing ternary metal structure etc.

Metal modified TiO_2 photocatalyst

Metal doping in a semiconductor photocatalyst significantly improves its hydrogen generation efficiency. Work function difference between the metal and semiconductor plays a vital role, generating the Schottky barrier (a potential energy barrier that arises at the semiconductor/metal interface) leading to improved photocatalytic performance of the catalyst. Several other factors contribute to this such as surface plasmon resonance (SPR), generation of new energy levels etc. The superior work function of noble metals and coinage metals such as silver (Ag), gold (Au), copper (Cu), platinum (Pt) and palladium (Pd) makes them suitable dopants for the TiO_2 based photocatalysts. As a result of doping, a Schottky barrier is formed between the Fermi energy level of the metal and the conduction band of TiO_2, which serves as a medium for transporting photogenerated electrons from the conduction band of TiO_2 to the metal, where reduction of proton to molecular hydrogen occurs. Again, this prevents the back transfer of electrons and maximises charge separation and minimises the charge recombination process. The higher the work function of doped metal the higher it's electron accepter ability which stabilizes the electron hole pair charge separation. In the case of the nanocomposite, the nanostructure's size also plays a significant role. Subramanian et al. reported the shifting of Fermi energy level of TiO_2/Au nanocomposites in different sizes of gold nanoparticles. The energies of Fermi level shifted to more negative values on decreasing size of the Au metal nanostructure, indicating greater electron accumulation which enhances the photocatalytic activity of the catalyst [21].

Another major factor is the SPR effect. This type of effect is observed both in the case of metal nanoparticle decorated TiO_2 and metal doped TiO_2. Irradiation of photocatalysts with the plasmon resonance frequency of doped metal (Ag, Au, Cu) generates an intense electrical field named hot spots, much stronger than the applied electromagnetic field, generates a higher amount of charge carriers facilitating the

photocatalytic hydrogen evolution reactions. Photoexcited electrons generated from metals such as Ag, Au through visible light irradiation transfer from metal to TiO_2. Whether the electron transfer occurs from metal to TiO_2 or TiO_2 to metal that depends on the nature of irradiated light, under visible light electron transfer occurs from metal to TiO_2 whereas electron transfer occurs from TiO_2 to metal under ultra violet light (see Fig. 5). Both types of electron transfers are possible under UV–visible light. Fang et al., [2012] reported the synthesis of mesoporous Au–TiO_2 nanostructures with significant photocatalytic water splitting activity in the presence of a sacrificial agent under visible light. The defect states lie in the TiO_2 matrix play minor role, whereas gold surface plasmons take the main lead in improving the visible-light photocatalytic activity of the reported nanostructure. Controlled light irradiation assists transfer of the dopant metal (Au) electron to the semiconductor (TiO_2), where reduction of water to hydrogen occurs [22].

New energy states created due to metal doping is also responsible for the suppression of the electron-hole pair recombination. Donor level generated above the valence band of TiO_2 or accepter level generated below the conduction band of TiO_2 as a result of metal doping successfully enhanced the photocatalytic performance of the catalyst (see Fig. 6) [23].

Non-metallic atom modified TiO_2 photocatalyst

Doping TiO_2 with non-metallic atoms or anions is another important way of improving photocatalytic activity of the catalyst in the visible region; the concept is relatively new. Different non-metal doped (nitrogen (N), fluorine (F), iodine (I), oxygen (O)) TiO_2 have been studied for photocatalytic hydrogen generation, which shows impressive results. Recent studies show that doping of TiO_2 with nitrogen relatively alters the band gap energy of the semiconductor photocatalyst. N 2p orbital of dopant atom interacts with the O 2p orbital of semiconductor TiO_2, thereby generating the gap states which reduces band gap energy of TiO_2. Such type of orbital mixing increases the energy of VB level of TiO_2, whereas the position of CB remains unaltered (Fig. 6). Under this condition, visible light irradiation can efficiently promote electron transfer from the uplifted valence band to the conduction band to generate molecular hydrogen. In addition, the charge recombination process is also suppressed. Non-metal ion doping seems more advantageous than metal doping because the generation of charge carrier recombination centres is disfavoured in the former case than in the latter [24]. Yongge Cao and his group reported the photocatalytic hydrogen generation activity of N-doped TiO_2 film. They observed that N doping in 4.91%, reduces the band gap of TiO_2 to 2.65 eV and hydrogen production rate increases to 601 mmol $g^{-1}h^{-1}$ [25]. The photocatalytic hydrogen generation activity of S-doped porous anatase TiO_2 nanostructure also has been studied which shows a hydrogen production rate of 163.9 mmol h^{-1} g^{-1} [26].

Apart from the above two types, co-doping of metal and nonmetals or metal/metal doping in TiO_2 efficiently narrows the band energy gaps and reduces the electron hole pair recombination rate, thereby producing several efficient photocatalysts for hydrogen generation. Coupling of TiO_2 (large band gap) with low band gap transition metal oxides and sulphides (zinc oxide, nickel oxide, iron oxide, bismuth sulfide, lead sulfide, cadmium sulfide etc.) also creates heterojunction which lowers the band gap of TiO_2 thus increases the visible light absorption efficiency. Reddy et al. reported the use of Bi_2O_3 as cocatalyst to enhance the photocatalytic hydrogen evolution activity of TiO_2 (Fig. 7(a)). Low cost Bi_2O_3 increases the H_2-production rate (920 μmol h^{-1}) by about 73 times compared to virgin TiO_2 [27]. Ren Jeng Wu and his group reported Pt-doped TiO_2–ZnO behaves as an efficient catalyst for water splitting with a high H_2 production rate (2150 mmol $h^{-1}g^{-1}$) and good stability. On irradiation of catalyst, electrons are excited to the conduction band from valence band and Platinum act as an electron transport medium where hydrogen evolution reaction occurs as shown in Fig. 7(b) [28]. Zhao et al. reported the use of three-dimensionally ordered macroporous structured

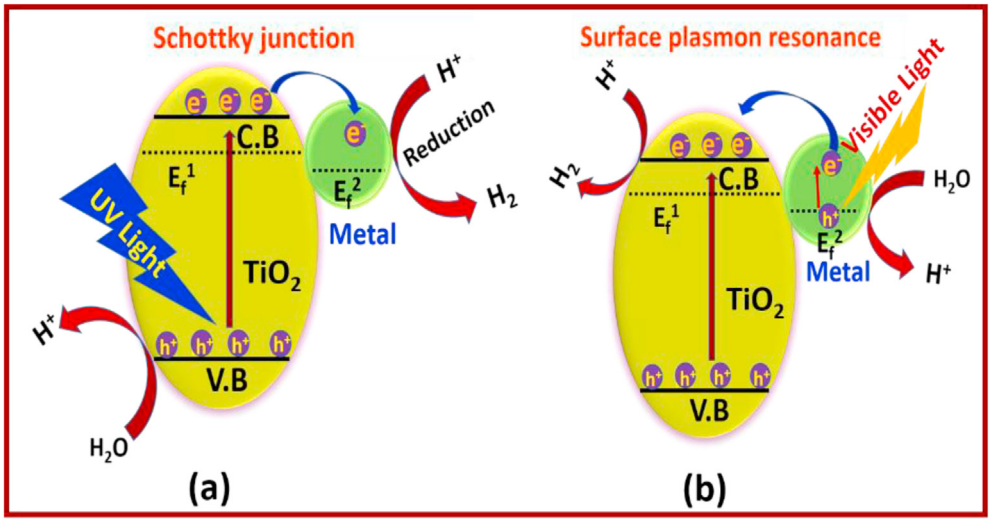

Fig. 5 – Schematic representation of (a) Schottky junction mediated charge transfer of metal/TiO_2 under UV light irradiation, (b) Surface plasmon resonance mediated charge transfer of metal/TiO_2 under visible light irradiation.

TiO_2–Au–CdS ternary photocatalyst for photocatalytic hydrogen generation [29]. Herein, Au and CdS nanoparticles synergistically improve the efficiency of the catalyst by enhancing light harvesting and using its mass transfer facilitation.

Graphitic carbon nitride-based photocatalysts

Graphitic carbon nitride (g-C_3N_4) is a narrow band gap (2.7 eV) visible light responsive metal free semiconductor first used by Domen and Antonietti groups for photocatalytic water splitting reaction. These are conjugated polymeric structures

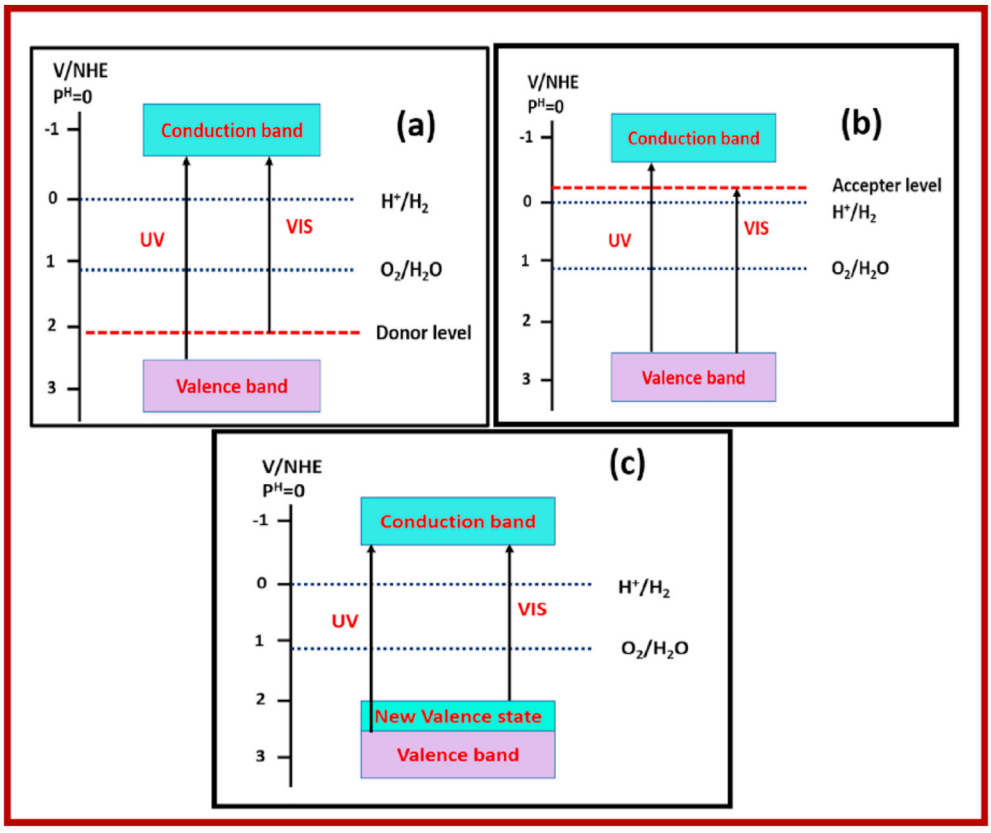

Fig. 6 – Schematic representation of (a) Donor, (b) Acceptor energy level generated due to metal doping and (c) Gap state generated due to the non-metal doping.

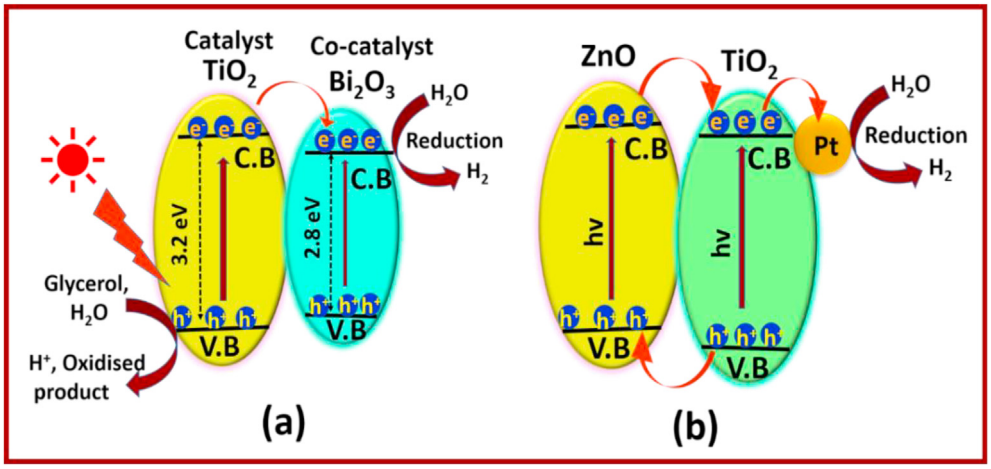

Fig. 7 – Schematic representation of (a) mechanism of photocatalytic hydrogen generation under solar irradiation utilizing Bi_2O_3@TiO_2 photo catalyst, (b) mechanism of photocatalytic hydrogen generation using Pt/TiO_2–ZnO photocatalyst.

containing tri-s-triazine units connected by planar amino groups, prepared via one step polymerization method using different starting materials such as urea, thiourea, cyanamide etc. Besides narrow band gap, low cost, non-toxicity and high photo corrosion resistance make them a suitable candidate for photocatalytic hydrogen evolution reaction. However low specific surface area and higher recombination rate of photogenerated electron-hole pairs limit their activity. In addition, incomplete polymerization of the precursors and structural deformation within the gC_3N_4 nanostructures generating blue shift of 2D nanostructure is a big issue. Shi Zhang Qiao and his group introduce a three-step technique comprising co-polymerization, surface activation and exfoliation for the synthesis of photo catalytically highly active gC_3N_4 nanostructure which shows a nearly 38 times increase in their hydrogen production rate in comparison to the virgin carbon nitride [30]. Rahman et al. reported the use of amorphous spongy carbon nitride structures with enhanced hydrogen production rate [31]. Other modifications such as metal and nonmetal doping, coupling with semiconductors etc. are introduced by the researchers to improve the photocatalytic activity of the catalysts. In case of gC_3N_4 absorption spectra is limited to ultraviolet and blue fraction of the solar spectrum. Doping with metal and nonmetals significantly alters the band gap of gC_3N_4, enhancing the visible light absorption. However, the problem of carrier recombination retains in the doped g-C_3N_4 structures. To improve photocatalyst efficiency, other surface area enhancement techniques such as soft and hard templating and copolymerization methods can be used.

Metal chalcogenide-based photocatalysts

Apart from TiO_2 and g-C_3N_4 based photocatalysts, different metal chalcogenides, metal chalcogenide based heterostructures and perovskites are studied for their photocatalytic hydrogen evolution activity. Chuan-Lu Yang and his group theoretically studied photocatalytic hydrogen generation activity of different heterostructures such as Z-scheme photocatalyst AuSe/SnS heterostructures with high STH efficiency (23.96%), HfS_2/SiSe heterostructure RuI_2/Sb_2S_3 heterostructure, and two-dimensional AuSe/SnSe heterostructures [32–35]. Apart from heterostructures different metal and nonmetal doped metal chalcogenides and perovskites such as Hg-doped ZnX (X = S, Se), Se-/In-doped $TlAsS_2$, Te-doped perovskite $NaTaO_3$, Chalcogens doped $BaTiO_3$ are also theoretically studied for their photocatalytic hydrogen generation activity [32,36–39]. These doped structures with modulated band gap show improved hydrogen generation efficiency. Different nanostructures and quantum dots are also theoretically studied for their hydrogen generation activity [40]. Liu et al. investigated the photocatalytic hydrogen evolution activity of halogen edge passivated antimonene nanoribbon by first-principles density functional theory calculations showing excellent catalytic activity [41]. Apart from theoretical study, different metal sulfide nanostructures and quantum dots are used experimentally for hydrogen generation. Different MoS_2-based catalyst such as MoS_2/CdS rod-like nanocomposites, NiCo nanoparticles supported on montmorillonite/MoS_2 heterostructure, and AgInZnS/MoS_2 hybrid show excellent photocatalytic activity [42–44]. Cavdar et al. reported synthesis of $ZnIn_2S_4$ microspheres/$CuInS_2$ quantum dots with improved hydrogen generation activity in the visible region [45]. Chen et al. utilizes metal free photocatalyst carbon quantum dots decorated with covalent triazine frameworks for hydrogen evolution [46]. Different types of photocatalyst systems are summarized below with their hydrogen production rate in Table 1.

Challenges and future perspectives

Although different systems have been studied for their photocatalytic activity, industrial production of hydrogen via solar water splitting suffers from several challenges such as low hydrogen generation efficiency and stability of the photocatalysts, low solar conversion efficiency, recyclability of the process etc. Most of the photocatalyst studied so far suffers from low solar to hydrogen (STH) conversion efficiency. Therefore, for practical application of the process, the following points must be considered. Firstly, prevention of recombination of photogenerated electrons and holes is necessary, which must migrate to the catalysts' surface for the occurrence of the reaction. Different photocatalyst systems have already been reported that minimize the recombination process such as Z-scheme photocatalysts, heterojunctions, p-n junctions but generation of these systems is time taking and requires several precautions. Therefore, a much deep understanding is needed for the development of easy techniques for generation of efficient catalysts. Another important factor is the generation of visible-light photocatalysts having suitable band gap and positions for hydrogen generation. Most semiconductor photocatalysts have a wide band gap and are only active in the ultraviolet region, preventing them from utilizing solar light. Development of pollution free, less expensive sacrificial agent is also a point of concern. Different industrial waste and organic pollutants can be used as sacrificial reagents, thereby achieving hydrogen generation and pollutant degradation simultaneously. In addition to this, different techno-economical details need further improvement such as the photoreactor design ie design of continuous feedstock and design of balance of system including piping, water supply, and panel structures. Maintenance of the reaction operational conditions and stability of the photocatalyst under reaction medium need to be further improved. Therefore, construction of a suitable low cost photoreactor with low photonic losses and high efficiency is very necessary. Solving the above issues can provide a path for industrial hydrogen generation via solar water splitting. Nevertheless, this system-level photocatalyst engineering is clearly a time-consuming process. Therefore, it is essential to deepen the understanding of structure-activity relationships and various photoredox mechanisms.

Table 1 – Summary of some metal and nonmetal modified photocatalysts for photocatalytic hydrogen evolution process.

Photocatalyst	Used light source	Hydrogen generation efficiency	Reference
Ag/TiO_2 nanotube	ultra-violet visible region	1.34 μmol $cm^{-2}h^{-1}$	[47]
Bimetallic Ag–Au on TiO_2 (Plasmonic)	visible-light-region	718 μmol h g^{-1} (quantum efficiency-3.3%)	[48]
Pt-doped TiO_2 nanocrystals	one a.m. 1.5G sunlight illumination	11200 μmol $h^{-1}g^{-1}$	[49]
Fe–Ni co-doped, Ag deposited anatase TiO_2	visible light region	793.86 μmol h^{-1} g^{-1} (λ > 400 nm for 6 h, energy efficiency is 0.25%)	[50]
Ru/TiO_2	500 W xenon lamp With a light cut-off filter UV light: (280–400 nm)	4.7 mmol h^{-1} g^{-1} (quantum efficiency-3.15%)	[51]
Au/g-C_3N_4 nanocomposite plasmonic photocatalysts	visible-light irradiation	532 μmol/3 h (23 times higher than virgin sample)	[52]
P-doped tubular g-C_3N_4 with surface carbon defects	a xenon 300 W lamp equipped with a 420-nm cut-off filter.	57 μmol h^{-1} (0.1 g catalyst)	[53]
B/Na co-doped porous g-C_3N_4 nanosheets	visible light λ > 400 nm	5971.51 μmol g^{-1} h^{-1}	[54]
copper doped carbon nitride nanotubes	300 W Xe lamp, λ > 420 nm	3.02 mmol h^{-1} g^{-1}	[55]
Ni nanoparticles modified N-doped g-C_3N_4	300 W Xe lamp, λ > 420 nm	1507 μmol g^{-1} h^{-1}	[56]
Oxygen doped g-C_3N_4 with nitrogen vacancy	visible light λ > 400 nm	2.20 mmol g^{-1} h^{-1}	[57]
Amorphous $Ni_2P_2O_7$ modified g-C_3N_4	visible light λ > 400 nm	474.7 μmol $h^{-1}g^{-1}$	[58]
$Ni_3B/Ni(OH)_2$ decorated g-C_3N_4 Nanosheets	visible light λ > 400 nm	352.43 μmol g^{-1} h^{-1}	[59]

Electrocatalytic hydrogen production through water splitting

Electrocatalytic hydrogen production via water splitting utilizing clean, renewable resources appears to be a promising strategy for the future energy portfolio. The sole importance of water as a starting material and combustion by-product in the cycle of hydrogen economy makes the process most efficient and sustainable. Paets van Troostwijk and the Deiman group reported the first electrolysis of water in 1789. Two half-cell reactions are involved in electrochemical water splitting; hydrogen evolution reaction (HER) occurring at the cathode and oxygen evolution reaction (OER) occurring at the anode.

Cathode reaction

$$2H^+ (aq) + 2e^- \rightarrow H_2$$

Anode reaction

$$2H_2O (l) \rightarrow 4H^+ (aq) + 4e^- + O_2 (g)$$

Overall water splitting reaction

$$2H_2O (l) \rightarrow 2H_2 (g) + O_2 (g)$$

Gives free energy change for the process appear to be $\Delta G^\circ = +237.2$ kJ mol^{-1} which corresponds to the electrode potential value of $\Delta E^\circ = 1.23$ V vs normal hydrogen electrode (NHE) for overall water splitting. For a standard hydrogen electrode, the reduction potential of H^+/H_2 couple is considered to be zero volt [3]. However, in common practice, excess potential over the thermodynamic potential is required to continue hydrogen evolution process due to sluggish reaction kinetics, known as overpotential for the process. Therefore, both the hydrogen and oxidation evolution processes require the use of efficient electrocatalysts which will lower the overpotential of the process and increase the rate of reactions. The present literature section focuses on electrocatalytic hydrogen production via water splitting. Appropriate hydrogen binding energy and gives free energy for hydrogen adsorption and desorption process make platinum (Pt) based catalysts and their derivatives the most efficient catalysts for HER. However, high cost and low availability of Pt and other precious platinum group metals on the earth's crust limit the broad application of Pt-based catalysts for H_2 production. Therefore, replacing noble metal-based catalysts with earth-abundant elements with superior catalytic activity is necessary for the practical implementation of hydrogen energy. Different transition metal-based oxides, chalcogenides, carbides, nitrides and phosphogenides have already been investigated for their electrocatalytic activity. The fundamental concept of electrocatalytic hydrogen evolution and the advancement of the use of various electrocatalysts are briefly discussed in the following section. Finally, the challenges and the future of hydrogen economy are discussed.

Fundamental concepts of electrocatalytic hydrogen evolution reaction

The mechanism of hydrogen evolution via water splitting involves three major steps for proton reduction either from acidic or alkaline water solutions. Initially, protons from the acidic or alkaline water solution get adsorbed on the electrocatalyst's surface via one-electron transfer from the electrode to produce adsorbed hydrogen atoms (H_{ad}) on active sites (M)

named as Volmer step. In the next step, hydrogen production may occur either from Heyrovsky step or Tafel step. Adsorbed hydrogen atoms (H_{ad}) may interact with another proton and by accepting an electron from the electrode produces hydrogen (Heyrovsky). Alternatively, two adsorbed hydrogen atoms in close vicinity may combine to produce molecular hydrogen named as Tafel step (see Figs. 8 and 9).

Step-1: electrochemical hydrogen adsorption (Volmer step)

$H_3O^+ + M + e^- \rightarrow M\text{-}H_{ad} + H_2O$ (acidic condition).

$H_2O + M + e^- \rightarrow M\text{-}H_{ad} + OH^-$ (alkaline condition)

Step-2: electrochemical hydrogen desorption (Heyrovsky step)

$M\text{-}H_{ad} + H_3O^+ + e^- \rightarrow H_2 + M + H_2O$ (acidic condition)

$M\text{-}H_{ad} + H_2O + e^- \rightarrow H_2 + M + HO^-$ (Alkaline condition)

Step-3: Recombination process (Tafel step)

$M\text{-}H_{ad} + M\text{-}H_{ad} \rightarrow H_2$ (both in acidic and alkaline conditions)

For a particular electrocatalyst which mechanism operates during the hydrogen evolution process i.e. Volmer-Heyrovsky or Volmer-Tafel, that can be known from the measurement of Tafel slope which is obtained by fitting the equation, $\eta = a + b\log(j)$ (where b is the Tafel slope, η is the overpotential, j is the current density, a is constant). If the recombination process is the rate determining step, then Tafel slope can be given by, $b = \frac{2.303RT}{2F} = 29\ mVdec^{-1}$, that low Tafel slope indicates Volmer-Tafel mechanism operates during the hydrogen evolution reaction. Whereas if Heyrovsky step is the rate determining, then Tafel slope $b = \frac{2.303RT}{3F} = 39\ mVdec^{-1}$, indicating Volmer- Heyrovsky mechanism is operating. A third case may arise where the initial step, that Volmer step is the rate determining. In such case, Tafel slope can be given by $b = \frac{2.303RT}{F} = 116 mVdec^{-1}$ [3].

Thermodynamic aspects

Sabatier principle (Sabatier, 1913; Che, 2013) states that "an ideal catalyst must bind to the reactant at an intermediate strength which is neither too weak nor too strong." If the catalyst binds the reactants strongly, then the hydrogen desorption process will be slow and reduces the rate of hydrogen generation. On the other hand, if catalyst/reactant

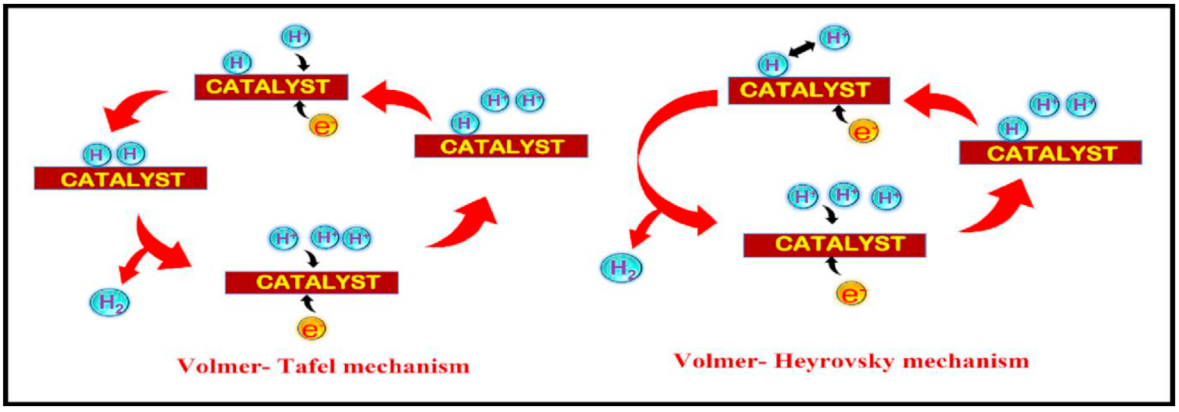

Fig. 8 – Schematic diagram of Volmer-Tafel and Volmer- Heyrovsky mechanism operating during hydrogen production under acidic condition

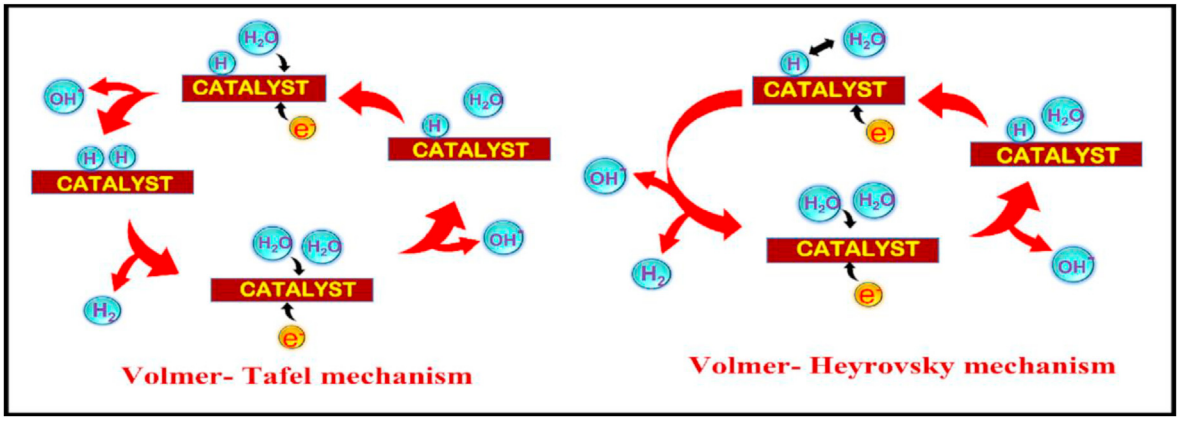

Fig. 9 – Schematic diagram of Volmer-Tafel and Volmer- Heyrovsky mechanism operating during hydrogen production under alkaline condition.

interaction is too weak, very few reactants get adsorb to the catalysts' surface, decreasing the hydrogen production rate. In terms of thermodynamic aspects by measuring gives free energy (ΔG) of the hydrogen evolution reaction, an idea about hydrogen adsorption and desorption energy can be obtained. The thermoneutral bonding situation where gives free energy (ΔG) for the reaction process becomes zero is considered to be ideal. Any deviation from this, either positive ΔG value or negative ΔG value makes the hydrogen evolution process thermodynamically unfavourable. Electrocatalyst will tune the free-energy landscape between the reactant and the product in a way that is advantageous for the hydrogen generation process. Parsons established a "volcano-type" curve which is obtained by plotting the hydrogen generation current density (j_0) value with respect to gives free energy of the process (ΔG). In this curve, the peak corresponds to zero ΔG, indicates ideal catalyst/reactant interaction, positive ΔG value indicates weak catalyst/reactant interaction and negative ΔG value indicates strong catalyst/reactant interaction. Further, Trasatti reported a volcano type curve obtained by plotting the metal hydrogen binding energy with the hydrogen generation current density [60].

Development in electrocatalytic hydrogen evolution

Noble metal-based electrocatalyst

Appropriate hydrogen binding energy and gives free energy of the hydrogen adsorption and desorption process make noble metals such as platinum (Pt), palladium (Pd), ruthenium (Ru), iridium (Ir) etc. as excellent catalysts for electrocatalytic hydrogen evolution reaction. These metals are positioned in the apex region of the volcano curve, where platinum occupies the peak position. Platinum is considered as most efficient electrocatalyst for hydrogen evolution reaction having "quasi-zero" onset overpotential with small Tafel slope [61]. However, high prices, low abundance and low stability in harsh electrolytic solutions limit their industrial application. Therefore, different modifications are introduced to lower their electrode mass loading while retaining high activity. Low platinum content electrocatalysts such as supported Pt nanostructures, Pt single-atom catalysts (SACs), Pt based alloy catalysts gain major attention in this respect. Conductive carbon matrix such as graphene act as an ideal matrix for platinum nanoparticles. Yan et al. reported the use of platinum nanoparticle decorated graphene nanospheres (Pt/GNs) electrocatalyst for hydrogen evolution reaction. The resultant electrocatalyst shows a low overpotential of 25 mV at the current density of 10 mA cm^{-2} in acidic solution [62]. Modification of carbon substrate with heteroatom further improves the efficiency of the catalyst. Huang et al. fabricated the CoMoPt/NC nanostructure with superior electrocatalytic activity in a broad P^H range (1–14) [63]. Different transition metal sulfides and hydroxides are also reported as potential support for platinum nanostructures [64,65]. Zexing Wu, Lei Wang and their group synthesized a low platinum content 2D-3D nanostructure with improved electrocatalytic activity [66]. Single platinum atom modification is also said to improve the platinum utilization efficiency of catalysts. Cheng et al. investigated the electrocatalytic activity of single platinum atom modified nitrogen-doped graphene which shows much enhanced catalytic activity. Partially unfilled density of states of 5d orbital of platinum atoms contributes to this enhanced electrocatalytic activity [67]. Facet engineering of platinum is another potential method of improving the catalytic activity of platinum based electrocatalysts. In an alkaline medium, the activity of different planes of Pt is found to be (110) plane > (100) plane > (111) plane [68]. Ruthenium (Ru) is inexpensive and has similar hydrogen binding energy (65 kcal/mol) like platinum making it a useful alternative. Electrocatalytic activity of Ru was further modified using different supports or synthesizing various ruthenium-based alloys. Chen et al. reported ruthenium nanostructure decorated graphene like carbon structure derived from silica as an excellent electrocatalyst for hydrogen evolution reaction which shows very low onset potential (3 mV) and small tafel slope (46 mV) in acidic solution [69]. A highly active p^H universal electrocatalyst Ru@C_4N was reported by Xing-Hua Xia and his co-workers for efficient hydrogen production from both acidic and alkaline solutions [70]. Bimetallic RuCu nanosheets also show great activity as p^H universal electrocatalyst for water splitting reaction [71]. Ru modified metal phosphides such as Ru, B co-doped nickel phosphide shows high electrocatalytic hydrogen generation activity in alkaline medium while Ru, B Co-doped iron phosphide electrocatalyst works in the wide P^H range [72,73]. In addition, Zexing Wu and his group reported different Ru modified metal oxides and metal hydroxides with improved electrocatalytic activity such as three dimensional Co_3O_4–RuO_2 hollow spheres, and Ru and CoFe hydroxide decorated phosphorus doped $CoFe_2O_4$ nanobelts [74,75]. Nearly top position of the Ir and Pd in HER volcano plot makes them viable platinum alternatives for electrocatalytic hydrogen evolution reaction. Particular (111) facets of Ir have moderate free energy of hydrogen adsorption/desorption process resulting in comparable electrocatalytic activity like (100) plane of Pt [76]. Javeed Mahmood and his group recently reported cage like organic network supported Ir nanoparticles show superior electrocatalytic hydrogen evolution activity with low overpotential and high stability both in acidic and alkaline solution [77]. Iridium based supported structures are also reported having good electrocatalytic activity such as macro porous nitrogen-doped carbon supported Ir/Mo phosphated structures show enhanced electrocatalytic activity (low overpotential of 14 mV at 10 mA/cm^2) in alkaline medium. The electronic structure of Ir is synergistically modulated by P and Mo thus facilitating the hydrogen generation [78]. Palladium has a similar size to Pt, a small lattice mismatch with Pt, and a high hydrogen adsorption capacity, which contributes to their electrocatalytic activity. The catalytic performance of Pd nanostructures is found to be largely affected by their dimensions and morphologies. Different morphology exposed different planes making a difference in their electronic structures thus changing catalytic activity. Supported Pd catalyst such as porous Pd nanostructure decorated carbon nitride shows good electrocatalytic activity and excellent stability in harsh acidic medium. Enhanced charge transfer, increased surface area and strong metal carbon bonding synergistically increase the activity of the catalyst [79].

Non noble metal-based electrocatalyst

In spite of having superior electrocatalytic activity, high cost and low abundance of noble metals motivated researchers to

exploit cheaper, earth-abundant electrocatalysts for hydrogen generation. In the biological system, hydrogenase and nitrogenase enzymes consist of iron (Fe), nickel (Ni), and molybdenum (Mo) as metals. They are devoid of noble metals; however, they effectively catalyse in vivo hydrogen evolution. Taking inspiration from this various transition metal-based oxides, chalcogenides, nitrides, carbides, phosphides, and so on are studied for their electrocatalytic activity [80]. Among them, molybdenum and tungsten-based materials have gained major attention. Molybdenum sulphide is the most extensively studied electrocatalyst for hydrogen evolution. In 2005, Norskov in his paper theoretically suggested molybdenum sulphide as potential electrocatalyst for hydrogen evolution since they have identical edge sites like nitrogenase enzyme which facilitates the catalytic reaction. Later Jaramillo and co-workers confirmed the active participation of MoS_2 edge sites experimentally [81]. Afterwards, different strategies have been used to enhance the electrocatalytic activity of MoS_2, such as (a) increasing catalytically active edge sites by reducing the size and changing morphologies, (b) introducing defects within the basal plane, thereby modulating the surface electronic structure so that free energy of hydrogen evolution process adjusted towards zero [82], (c) doping of metals (noble metals and non-noble metals) and nonmetals (hetero atoms) within MoS_2 matrix, (d) tuning of conventional semiconducting 2H phase of MoS_2 to conducting metallic 1T and 1T′ phase thereby boosting the charge transfer kinetics, (e) coupling with carbon based conductive materials (carbon nanotube, graphene etc.) and different metal oxides, carbides, sulfides thereby producing heterostructures with higher conductivity and good electrocatalytic activity. Santanu Das and his co-workers recently published a mini review regarding electrocatalytic hydrogen generation activity of metallic 1T MoS_2 [83]. The catalytic activity of metallic 1T phase of MoS_2 is comparable to platinum but it suffers from stability issues. Different techniques are used for the synthesis of meta-stable 1T phase of MoS_2 from 2H MoS_2 such as thermal treatment, atomic doping, and creating sulfur vacancy. However, reversibility of metallic 1T phase of MoS_2 to 2H phase makes the use of reported catalyst much more challenging. Similarity in structure with MoS_2 makes tungsten-based chalcogenides, tungsten sulfides (WS_2) and tungsten selenides (WSe_2) catalytically active for hydrogen generation. Manish Chhowalla and his co-workers synthesized strained metallic 1T (octahedral) phase WS_2 with excellent electrocatalytic activity via chemical exfoliation. Xingji Li and his group recently reported the synthesis of selenium-deficient 1T-WSe_2 phase from the 2H–WSe_2 phase via electron beam irradiation with enhanced electrocatalytic activity [84]. Doping of tungsten chalcogenides also significantly improves their catalytic activity. Other transition metal (cobalt, iron, copper, nickel) based sulfides and selenides are also reported to have comparable electrocatalytic activity. Suib et al. reported mesoporous iron sulfide prepared by sol-gel method shows good electrocatalytic activity in strong alkaline medium with low onset potential and good stability [85]. Recently petal-like iron sulfide/tungsten sulfide heterojunction nanosheets reported with superior electrocatalytic activity in acidic solution. Different nickel sulfide phases (Ni_3S_2, NiS, NiS_2) have been studied for their electrocatalytic activity. Among them, Ni_3S_2 shows the best catalytic activity under an alkaline medium [86]. Different transition metal doped metal sulfides also show improved catalytic activity due to modulation of gives free energy of the process originating from metal doping [87]. In addition, Binary and ternary transition metal chalcogenides have improved electrocatalytic activity due to the abundant redox rich sites. Excellent redox reversibility, improved electronic structure and high electrical conductivity make them potential candidates for hydrogen generation. Binary iron-nickel sulfide ultrathin nanosheet shows good electrocatalytic activity with lower overpotential (105 mV at 10 mA/cm^2) and small Tafel slope (40 mV/dec) [88]. Several attempts have been made for further improvement of these ternary metal chalcogenides such as structural investigation, morphology modulation, and generation of hybrids. Hota et al. reported neutral medium electrocatalytic activity of three different phases of copper antimony sulfide nanostructures namely chalcostibite, skinnerite, and famatinite. The chalcostibite phase shows the best catalytic activity among them due to the presence of easily accessible antimony (Sb) lone pair electron (see Fig. 10) [89]. Erum Pervaiz and his group recently summarize the electrocatalytic hydrogen generation activity of different morphologies of nickel cobalt sulphide and their hybrids with improved catalytic activity [90]. Li et al. (2019) reported the synthesis of cauliflower-like $CoNi_ySx$@PPy composite which shows enhanced catalytic activity in alkaline solution [91]. Whereas copper nickel tin sulphide decorated reduced graphene oxide composite shows promising catalytic activity in harsh acidic solution [92].

Different transition metal phosphides and carbides also gain considerable interest as potential candidates for hydrogen generation via water splitting. Motivated by [NiFe] hydrogenase, Liu and Rodriguez suggested nickel phosphides having (001) planes as potential candidates for hydrogen generation. Later, Fe_2P-type Ni_2P structures are also reported as efficient electrocatalysts. Different transition metal doping within nickel phosphides also significantly improves their electrocatalytic activity by increasing their hydrogen coverages. Among different metal carbides, molybdenum carbide (Mo_2C) gains major attention as effective electrocatalyst due to its Pt-like electronic configuration. DFT study suggested that molybdenum d orbitals and carbon s, p orbitals hybridize together broadening the d-band structure of molybdenum carbide thus generating Pt like d band structure. Different Mo_2C nanostructures, carbon encapsulated molybdenum carbides, doped molybdenum carbides show excellent catalytic activity. Other carbides such as tungsten carbide, cobalt carbide, nickel carbide and bimetallic carbides are also studied for their catalytic activity [93]. Different metal borides and nitrides are also investigated for their catalytic activity for hydrogen generation. Various heterostructures and hybrids also show excellent catalytic activity due to enhanced catalytic active centres synergistically derived from the heterogeneous interfaces which make the hydrogen adsorption-desorption process much more feasible. Lifang Jiao and his group recently (2022) reported that Ni_2P/NiMoP heterostructure shows excellent catalytic activity with low overpotential and long-term stability [94]. $Ni_{0.85}Se/Ni_3S_2$ heterostructure is also reported to have good electrocatalytic activity in alkaline medium [95]. Metal hybrid embedded carbon matrix such as N, S, O-doped carbon sheets coated CoP/

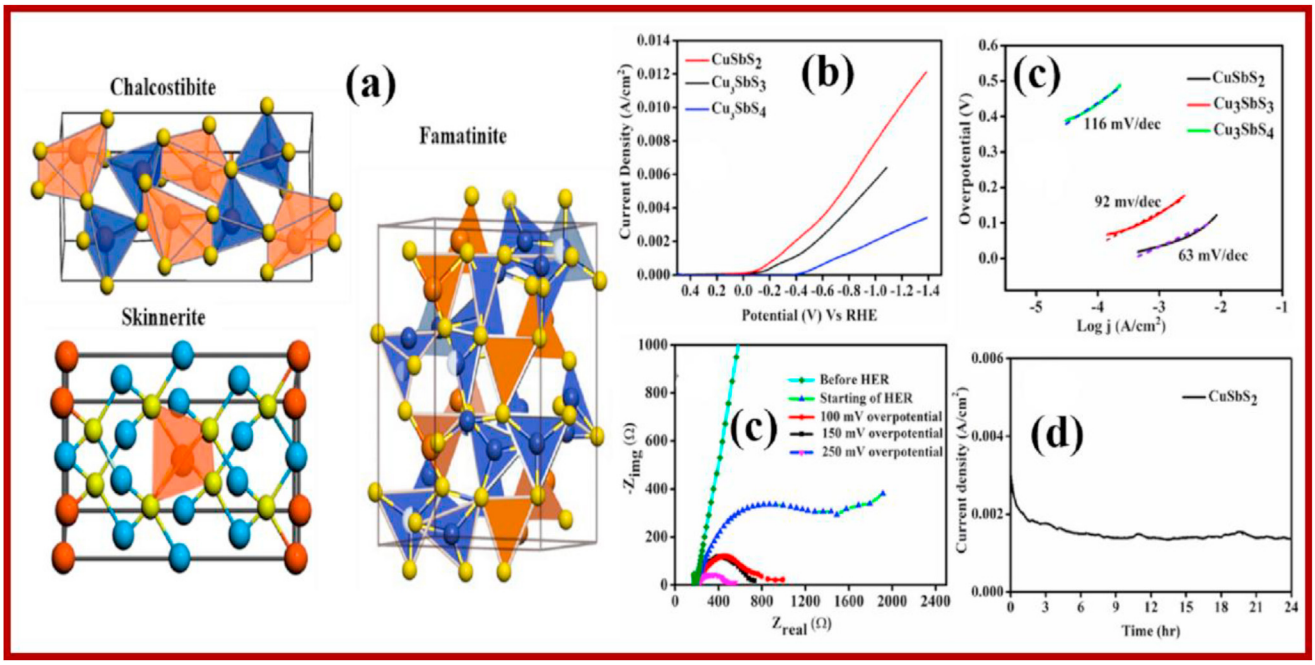

Fig. 10 – (a) Schematic representation of crystal structures of different phases of copper antimony sulphide, Chalcostibite ($CuSbS_2$), Famatinite (Cu_3SbS_4), and Skinnerite (Cu_3SbS_3) phases, (b) HER polarization curves of $CuSbS_2$, Cu_3SbS_3 and Cu_3SbS_4 nanostructures, (c) Tafel plots corresponding to the nanostructures, (d) Nyquist plots measured during the hydrogen evolution of $CuSbS_2$ system, and (e) neutral medium stability measurement of $CuSbS_2$ system.

Co_3S_4, N, P-codoped molybdenum carbide nanoparticles loaded into N, P-codoped graphene, magic hybrid constitute of $CoPt_3$ and CoPt nanoparticles supported on N doped carbon, Carbon supported Ni_3N/Ni heterostructure etc. are also reported to have good electrocatalytic activity [96–99]. Metal hybrid provides a large number of active centres which adsorbs large number of hydrogen ions whereas carbon matrix improves the electrical conductivity of the system making electron transport faster, thus improving the electrocatalytic activity of the catalyst. Apart from this, hydrogen generation through metal cluster mediated water splitting is also studied extensively. Chuan-Lu Yang and his group theoretically studied direct water splitting using different cluster compounds such as Al_6Si cluster, Pt_7 cluster, and Al_6Cu cluster [100–103]. Cluster compounds such as thiomolybdate $[Mo_3S_{13}]^{2-}$ clusters, and supported incomplete cubane-type $[Mo_3S_4]^{4+}$ also show good catalytic activity towards hydrogen generations [104,105].

Metal-free electrocatalysts

Over the years, various metal-based electrocatalysts have been investigated for their electrocatalytic activity. However, in recent times metal-free carbon-based materials have gained significant attention due to their superior conductivity, good stability under harsh acidic/alkaline conditions and changeable molecular structure. Carbon based substrates are chosen that satisfy the criteria of active centres for hydrogen adsorption and good conductivity for charge transportation. In 2014 Mingwei Chen and his group reported nitrogen, sulfur co-doped nanoporous graphene as an efficient metal-free electrocatalyst for hydrogen generation reaction. In this case, geometrical lattice defects originated due to nitrogen and sulfur doping modulating the process's free energy, thereby enhancing the catalyst's electrocatalytic activity [106]. Different dual hetero atom co-doped graphene structures such as nitrogen-phosphorous modified graphene and nitrogen-fluorine modified graphene are also reported as efficient catalysts for hydrogen generation. Besides different heteroatom doped graphene, heteroatom doped carbon nanotubes and functionalized carbon nanotubes are also reported as efficient catalysts for hydrogen evolution. Ethylenediamine-functionalized multiwalled carbon nanotube shows promising electrocatalytic activity with low onset potential (150 mV) and high faradaic efficiency (94%) [107]. Shi-Zhang Qiao and his group reported the synthesis of nitrogen, sulfur co-doped carbon nanotube derived from Polydopamine for overall water splitting. Another important class of carbon-free electrocatalysts is graphitic carbon nitride based electrocatalysts. These are doped with different p block elements or coupled with doped graphene to modulate their electronic properties for efficient hydrogen generation. Shi Zhang Qiao and his group reported the use of graphitic-carbon nitride (g-C_3N_4)/nitrogen-doped graphene heterostructure as an efficient catalyst for hydrogen generation [108]. Very recently metal-free covalent organic polymers are gaining interest for hydrogen generation. Pradhan et al. reported the synthesis of 1,3,5-tris(4-formylphenyl) benzene-based porous covalent polymer, which shows excellent electrocatalytic activity with low over potential (185 mV at 10 mA cm^{-2}) and small Tafel slope (68.5 mV $decade^{-1}$) [109]. Few metal-based and metal-free electrocatalysts are summarized below (see Table 2).

Table 2 – Summary of few metal based and metal free electrocatalysts.

Electrocatalyst	Electrolyte	Overpotential	Tafel slop mV dec^{-1}	Reference
Pt6@hydrogel	0.5 M H_2SO_4	45 mV at 10 mA cm^{-2}	52 mV dec^{-1}	[110]
Ru@C_2N	0.5 M H_2SO_4	25 mV at 10 mA cm^{-2}	30 mV dec^{-1}	[111]
Ru@MWCNT	0.5 M H_2SO_4	13 mV at 10 mA cm^{-2}	27 mV dec^{-1}	[112]
1T $MoSe_2$	0.5 M H_2SO_4	152 mV at 10 mA cm^{-2}	52 mV dec^{-1}	[113]
MoO_2 NSs	1.0 M KOH	27 mV at 10 mA cm^{-2}	41 mV dec^{-1}	[114]
$_{CuCoO}$ NWs	1.0 M KOH	85 mV at 10 mA cm^{-2}	108 mV dec^{-1}	[115]
MoN-NC NPs	0.5 M H_2SO_4	62 mV at 10 mA cm^{-2}	54 mV dec^{-1}	[116]
NiMoN	1.0 M KOH	109 mV at 10 mA cm^{-2}	165 mV dec^{-1}	[117]
Porous 2H MoS_2	0.5 M H_2SO_4	218 mV at 10 mA cm^{-2}	62 mV dec^{-1}	[118]
3D graphene	0.5 M H_2SO_4	163 mV at 10 mA cm^{-2}	89 mV dec^{-1}	[119]
Co9S4P4 Pentlandit	Neutral solution	84 mV at 10 mA cm^{-2}	106 mV dec^{-1}	[120]
NiRuIr@Graphene nanohybrid	Neutral solution	100 mV at 10 mA cm^{-2}	72 mV dec^{-1}	[121]

Challenges and future perspectives

Different metal and non-metal based electrocatalysts are widely studied for electrocatalytic hydrogen generation. However, their practical application for industrial hydrogen production suffers from several limitations. A major problem is the generation of low cost, highly efficient catalysts for industrial hydrogen production. Although various noble metal-free electrocatalysts have been investigated for electrocatalytic hydrogen generation, only a few of them exhibit comparable efficiency to platinum group metals. They also suffer from stability and durability issues. Therefore, exploration of less expansive earth-abundant electrocatalysts with high activity and stability under a wide p^H range is recommended. It is necessary to have a detailed mechanistic understanding of noble metal free hydrogen evolution in order to design low-cost, efficient electrocatalysts. Although the DFT study gives an idea about the mechanism of electrocatalytic water splitting theoretically, experimental situation often differs from theory. And the comprehensive mechanistic study is essential. In addition, metal hydrogen binding energy, which is a prime deciding factor for the electrocatalytic activity of catalyst, evaluated theoretically under ideal conditions. The practical situation differs from the ideal and therefore discovery of a novel experimental method for the evaluation of metal hydrogen binding energy is much needed. Moreover, the use of Pt-based counter electrodes during determination of electrocatalytic activity of a catalyst in a three-electrode cell should be avoided unless there is an ion-exchange membrane. Since the electrochemical dissolution of platinum may highly affect the measured activity of catalyst gives misleading information. Carbon based electrodes are highly recommended for this purpose. During electrocatalytic hydrogen generation, the electrochemical cell should be designed appropriately to reduce hydrogen purification costs. Solving these issues gives a path for industrial hydrogen production via electrocatalytic water splitting.

Conclusion

The current literature summarizes various low cost and high performance electrocatalysts and photocatalysts reported in recent years for hydrogen fuel generation via water splitting. The mechanism of hydrogen production via water splitting using various photocatalysts and electrocatalysts is also thoroughly discussed. Advancement of two main photocatalysts TiO_2 and gC_3N_4 in photocatalytic hydrogen generation are discussed with different strategies adopted to improve their catalytic activity. Various techniques used for the generation of noble metal free efficient electrocatalyst are discussed, such as enhancing catalytic active centres by modulating the morphology and electronic structure of catalyst, coupling with conductive substance thereby producing heterostructures with improved charge transport kinetics, doping with different metal and nonmetal atoms thereby optimizing the free energy change for the hydrogen generation reaction etc. Finally, challenges and future of hydrogen production via electrocatalytic and photocatalytic water splitting are discussed. We hope this literature will provide a good understanding to the reader regarding green fuel hydrogen generation methods and will be helpful in designing efficient catalysts for electrocatalytic and photocatalytic hydrogen generation.

Declaration of competing interest

The authors declare that they have no known competing financial interests or personal relationships that could have appeared to influence the work reported in this paper.

Acknowledgments

Funding from Ministry of Mines (Project No. Met4-14/19/2021), and research fellowship from CSIR (RA & SRF.) Govt. of India, are gratefully acknowledged.

REFERENCES

[1] Ji M, Wang J. Review and comparison of various hydrogen production methods based on costs and life cycle impact assessment indicators. Int J Hydrogen Energy 2021;46:38612–35.
[2] Zhu J, Hu L, Zhao P, Lee LY, Wong KY. Recent advances in electrocatalytic hydrogen evolution using nanoparticles. Chem Rev 2019;120:851–918.

[3] Zhao W, Chen Z, Yang X, Qian X, Liu C, Zhou D, Sun T, Zhang M, Wei G, Dissanayake PD, Ok YS. Recent advances in photocatalytic hydrogen evolution with high-performance catalysts without precious metals. Renew Sustain Energy Rev 2020;132:110040.
[4] Sun L, Han L, Huang J, Luo X, Li X. Single-atom catalysts for photocatalytic hydrogen evolution: a review. Int J Hydrogen Energy 2022;47:17583–99.
[5] Anwar S, Khan F, Zhang Y, Djire A. Recent development in electrocatalysts for hydrogen production through water electrolysis. Int J Hydrogen Energy 2021;46:32284–317.
[6] Yao Y, Gao X, Meng X. Recent advances on electrocatalytic and photocatalytic seawater splitting for hydrogen evolution. Int J Hydrogen Energy 2021;46:9087–100.
[7] Yanalak G, Aljabour A, Aslan E, Ozel F, Patir IH. A systematic comparative study of the efficient co-catalyst-free photocatalytic hydrogen evolution by transition metal oxide nanofibers. Int J Hydrogen Energy 2018;43:17185–94.
[8] Eftekhari A. Electrocatalysts for hydrogen evolution reaction. Int J Hydrogen Energy 2017;42:11053–77.
[9] Zhao Y, Zhang X, Wang T, Song T, Yang P. Fabrication of rGO/CdS@2H, 1T, amorphous MoS_2 heterostructure for enhanced photocatalytic and electrocatalytic activity. Int J Hydrogen Energy 2020;45:21409–21.
[10] Fujishima A, Honda K. Electrochemical photolysis of water at a semiconductor electrode. Nature 1972;238:37–8.
[11] Wen X, Sun N, Tan Y, Wang W, Yan C, Wang H. One-step synthesis of petals-like graphitic carbon nitride nanosheets with triazole defects for highly improved photocatalytic hydrogen production. Int J Hydrogen Energy 2019;44:2675–84.
[12] Vyas Y, Chundawat P, Dharmendra D, Punjabi PB, Ameta C. Review on hydrogen production photocatalytically using carbon quantum dots: future fuel. Int J Hydrogen Energy 2021;46:37208–41.
[13] Shiraz HG, Crispin X, Berggren M. Transition metal sulfides for electrochemical hydrogen evolution. Int J Hydrogen Energy 2021;46:24060–77.
[14] Ma J, Wei H, Liu Y, Ren X, Li Y, Wang F, Han X, Xu E, Cao X, Wang G, Ren F. Application of Co_3O_4-based materials in electrocatalytic hydrogen evolution reaction: a review. Int J Hydrogen Energy 2020;45:21205–20.
[15] Fajrina N, Tahir M. A critical review in strategies to improve photocatalytic water splitting towards hydrogen production. Int J Hydrogen Energy 2019;44:540–77.
[16] Rahman MZ, Kibria MG, Mullins CB. Metal-free photocatalysts for hydrogen evolution. Chem Soc Rev 2020;49:1887–931.
[17] Fu CF, Sun J, Luo Q, Li X, Hu W, Yang J. Intrinsic electric fields in two-dimensional materials boost the solar-to-hydrogen efficiency for photocatalytic water splitting. Nano Lett 2018;18:6312–7.
[18] Qiao NH, Yang CL, Wang MS, Ma XG. Two-dimensional TeX (X= C, Si, Ge) monolayers with strong intrinsic electric field for efficiency hydrogen evolution reaction. Surface Interfac 2022;31:102011.
[19] Zhang H, Liu F, Wu H, Cao X, Sun J, Lei W. In situ synthesis of gC_3N_4/TiO_2 heterostructures with enhanced photocatalytic hydrogen evolution under visible light. RSC Adv 2017;7:40327–33.
[20] Kumaravel V, Mathew S, Bartlett J, Pillai SC. Photocatalytic hydrogen production using metal doped TiO_2: a review of recent advances. Appl Catal B Environ 2019;244:1021–64.
[21] Subramanian V, Wolf EE, Kamat PV. Catalysis with TiO_2/gold nanocomposites. Effect of metal particle size on the Fermi level equilibration. J Am Chem Soc 2004;126:4943–50.
[22] Fang J, Cao SW, Wang Z, Shahjamali MM, Loo SC, Barber J, Xue C. Mesoporous plasmonic Au–TiO_2 nanocomposites for efficient visible-light-driven photocatalytic water reduction. Int J Hydrogen Energy 2012;37:17853–61.
[23] Martha S, Sahoo PC, Parida KM. Martha S, Sahoo PC, Parida KM. An overview on visible light responsive metal oxide based photocatalysts for hydrogen energy production. RSC Adv 2015;5:61535–53.
[24] Wang YY, Chen YX, Barakat T, Zeng YJ, Liu J, Siffert S, Su BL. Recent advances in non-metal doped titania for solar-driven photocatalytic/photoelectrochemical water-splitting. J Energy Chem 2022;66:529–59.
[25] Wang C, Hu Q, Huang J, Wu L, Deng Z, Liu Z, Liu Y, Cao Y. Efficient hydrogen production by photocatalytic water splitting using N-doped TiO_2 film. Appl Surf Sci 2013;283:188–92.
[26] Xing Z, Li Z, Wu X, Wang G, Zhou W. In-situ S-doped porous anatase TiO_2 nanopillars for high-efficient visible-light photocatalytic hydrogen evolution. Int J Hydrogen Energy 2016;41:1535–41.
[27] Reddy NL, Emin S, Valant M, Shankar MV. Nanostructured Bi_2O_3@ TiO_2 photocatalyst for enhanced hydrogen production. Int J Hydrogen Energy 2017;42:6627–36.
[28] Xie MY, Su KY, Peng XY, Wu RJ, Chavali M, Chang WC. Hydrogen production by photocatalytic water-splitting on Pt-doped TiO_2–ZnO under visible light. J Taiwan Inst Chem Eng 2017;70:161–7.
[29] Zhao H, Wu M, Liu J, Deng Z, Li Y, Su BL. Synergistic promotion of solar-driven H_2 generation by three-dimensionally ordered macroporous structured TiO_2-Au-CdS ternary photocatalyst. Appl Catal B Environ 2016;184:182–90.
[30] Rahman MZ, Ran J, Tang Y, Jaroniec M, Qiao SZ. Surface activated carbon nitride nanosheets with optimized electro-optical properties for highly efficient photocatalytic hydrogen production. J Mater Chem A 2016;4:2445–52.
[31] Rahman MZ, Tapping PC, Kee TW, Smernik R, Spooner N, Moffatt J, Tang Y, Davey K, Qiao SZ. A benchmark quantum yield for water photoreduction on amorphous carbon nitride. Adv Funct Mater 2017;27:1702384.
[32] Yin QK, Yang CL, Wang MS, Ma XG. Two-dimensional heterostructures of AuSe/SnS for the photocatalytic hydrogen evolution reaction with a Z-scheme. J Mater Chem C 2021;9:12231–8.
[33] Zhang CF, Yang CL, Wang MS, Ma XG. Z-Scheme photocatalytic solar-energy-to-hydrogen conversion driven by the HfS_2/SiSe heterostructure. J Mater Chem C 2022;10:5474–81.
[34] Wang F, Yang CL, Wang MS, Ma X. Photocatalytic hydrogen evolution reaction with high solar-to-hydrogen efficiency driven by the Sb_2S_3 monolayer and RuI_2/Sb_2S_3 heterostructure with solar light. J Power Sources 2022;532:231352.
[35] Yin QK, Yang CL, Wang MS, Ma XG. Two-dimensional AuSe/SnSe heterostructure for solar photocatalytic hydrogen evolution reaction with Z-scheme. Sol Energy Mater Sol Cell 2022;247:111940.
[36] Huang HC, Yang CL, Wang MS, Ma XG. Pristine and Se-/In-doped $TlAsS_2$ enhance the solar energy-driven water splitting for hydrogen generation. Int J Hydrogen Energy 2017;42:15464–70.
[37] Huang HC, Yang CL, Wang MS, Ma XG. Optical absorption enhancement of Hg-doped ZnX (X= S, Se) for hydrogen production from water splitting driven by solar energy. Vacuum 2018;157:36–44.
[38] Liu YL, Yang CL, Wang MS, Ma XG, Yi YG. Te-doped perovskite $NaTaO_3$ as a promising photocatalytic material for hydrogen production from water splitting driven by visible light. Mater Res Bull 2018;107:125–31.

[39] Huang HC, Yang CL, Wang MS, Ma XG. Chalcogens doped $BaTiO_3$ for visible light photocatalytic hydrogen production from water splitting. Spectrochim Acta Mol Biomol Spectrosc 2019;208:65–72.
[40] Liu YL, Yang CL, Wang MS, Ma XG, Yi YG. Theoretical insight into the optoelectronic properties of lead-free perovskite derivatives of $Cs_3Sb_2X_9$ (X= Cl, Br, I). J Mater Sci 2019;54:4732–41.
[41] Liu M, Yang CL, Wang MS, Ma XG. Halogen edge-passivated antimonene nanoribbons for photocatalytic hydrogen evolution reaction with high solar-to-hydrogen conversion. J Phys Chem C 2021;125:21341–51.
[42] Zhao H, Fu H, Yang X, Xiong S, Han D, An X. MoS_2/CdS rod-like nanocomposites as high-performance visible light photocatalyst for water splitting photocatalytic hydrogen production. Int J Hydrogen Energy 2022;47:8247–60.
[43] Xu J, Gao J, Wang W, Wang C, Wang L. Noble metal-free NiCo nanoparticles supported on montmorillonite/MoS_2 heterostructure as an efficient UV–visible light-driven photocatalyst for hydrogen evolution. Int J Hydrogen Energy 2018;43:1375–85.
[44] Huang T, Chen W, Liu TY, Hao QL, Liu XH. Hybrid of AgInZnS and MoS_2 as efficient visible-light driven photocatalyst for hydrogen production. Int J Hydrogen Energy 2017;42:12254–61.
[45] Cavdar O, Malankowska A, Amgar D, Mazierski P, Łuczak J, Lisowski W, Zaleska-Medynska A. Remarkable visible-light induced hydrogen generation with $ZnIn_2S_4$ microspheres/$CuInS_2$ quantum dots photocatalytic system. Int J Hydrogen Energy 2021;46:486–98.
[46] Chen Y, Huang G, Gao Y, Chen Q, Bi J. Up-conversion fluorescent carbon quantum dots decorated covalent triazine frameworks as efficient metal-free photocatalyst for hydrogen evolution. Int J Hydrogen Energy 2022;47:8739–48.
[47] Wu F, Hu X, Fan J, Liu E, Sun T, Kang L, Hou W, Zhu C, Liu H. Photocatalytic activity of Ag/TiO_2 nanotube arrays enhanced by surface plasmon resonance and application in hydrogen evolution by water splitting. Plasmonics 2013;8:501–8.
[48] Patra KK, Gopinath CS. Bimetallic and plasmonic Ag–Au on TiO_2 for solar water splitting: an active nanocomposite for entire visible light region absorption. ChemCatChem 2016;8:3294–311.
[49] Banerjee B, Amoli V, Maurya A, Sinha AK, Bhaumik A. Green synthesis of Pt-doped TiO_2 nanocrystals with exposed (001) facets and mesoscopic void space for photo-splitting of water under solar irradiation. Nanoscale 2015;7:10504–12.
[50] Sun T, Liu E, Liang X, Hu X, Fan J. Enhanced hydrogen evolution from water splitting using Fe-Ni codoped and Ag deposited anatase TiO_2 synthesized by solvothermal method. Appl Surf Sci 2015;347:696–705.
[51] Gu Q, Gao Z, Yu S, Xue C. Constructing Ru/TiO_2 heteronanostructures toward enhanced photocatalytic water splitting via a RuO_2/TiO_2 heterojunction and Ru/TiO_2 Schottky junction. Adv Mater Interfac 2016;3:1500631.
[52] Samanta S, Martha S, Parida K. Facile synthesis of Au/g-C_3N_4 nanocomposites: an inorganic/organic hybrid plasmonic photocatalyst with enhanced hydrogen gas evolution under visible-light irradiation. ChemCatChem 2014;6:1453–62.
[53] Guo S, Tang Y, Xie Y, Tian C, Feng Q, Zhou W, Jiang B. P-doped tubular g-C_3N_4 with surface carbon defects: universal synthesis and enhanced visible-light photocatalytic hydrogen production. Appl Catal B Environ 2017;218:664–71.
[54] Chi X, Liu F, Gao Y, Song J, Guan R, Yuan H. An efficient B/Na co-doped porous g-C_3N_4 nanosheets photocatalyst with enhanced photocatalytic hydrogen evolution and degradation of tetracycline under visible light. Appl Surf Sci 2022;576:151837.
[55] Yan X, Jia Z, Che H, Chen S, Hu P, Wang J, Wang L. A selective ion replacement strategy for the synthesis of copper doped carbon nitride nanotubes with improved photocatalytic hydrogen evolution. Appl Catal B Environ 2018;234:19–25.
[56] Deng P, Gan M, Zhang X, Li Z, Hou Y. Non-noble-metal Ni nanoparticles modified N-doped g-C_3N_4 for efficient photocatalytic hydrogen evolution. Int J Hydrogen Energy 2019;44:30084–92.
[57] Tang H, Xia Z, Chen R, Liu Q, Zhou T. Oxygen doped g-C_3N_4 with nitrogen vacancy for enhanced photocatalytic hydrogen evolution. Chem Asian J 2020;15:3456–61.
[58] Wulan BR, Yi SS, Li SJ, Duan YX, Yan JM, Jiang Q. Amorphous nickel pyrophosphate modified graphitic carbon nitride: an efficient photocatalyst for hydrogen generation from water splitting. Appl Catal B Environ 2018;231:43–50.
[59] Feng J, Zhang D, Zhou H, Pi M, Wang X, Chen S. Coupling P nanostructures with P-doped g-C_3N_4 as efficient visible light photocatalysts for H_2 evolution and RhB degradation. ACS Sustainable Chem Eng 2018;6:6342–9.
[60] Ooka H, Huang J, Exner KS. The sabatier principle in electrocatalysis: basics, limitations, and extensions. Front Energy Res 2021;9:155.
[61] Greeley J, Jaramillo TF, Bonde J, Chorkendorff IB, Nørskov JK. Computational high-throughput screening of electrocatalytic materials for hydrogen evolution. Nat Mater 2006;5:909–13.
[62] Yan X, Li H, Sun J, Liu P, Zhang H, Xu B, Guo J. Pt nanoparticles decorated high-defective graphene nanospheres as highly efficient catalysts for the hydrogen evolution reaction. Carbon 2018;137:405–10.
[63] Huang WH, Li XM, Yu DY, Yang XF, Wang LF, Liu PB, Zhang J. CoMo-bimetallic N-doped porous carbon materials embedded with highly dispersed Pt nanoparticles as pH-universal hydrogen evolution reaction electrocatalysts. Nanoscale 2020;12:19804–13.
[64] Yu W, Chen Z, Zhao Y, Gao Y, Xiao W, Dong B, Wu Z, Wang L. An in situ generated 3D porous nanostructure on 2D nanosheets to boost the oxygen evolution reaction for water-splitting. Nanoscale 2022;14:4566–72.
[65] Li Z, Ge R, Su J, Chen L. Recent progress in low Pt content electrocatalysts for hydrogen evolution reaction. Adv Mater Interfac 2020;7:2000396.
[66] Chen Z, Liu D, Gao Y, Zhao Y, Xiao W, Xu G, Ma T, Wu Z, Wang L. Corrosive-coordinate engineering to construct 2D-3D nanostructure with trace Pt as efficient bifunctional electrocatalyst for overall water splitting. Sci China Mater 2022;65:1217–24.
[67] Cheng N, Stambula S, Wang D, Banis MN, Liu J, Riese A, Xiao B, Li R, Sham TK, Liu LM, Botton GA. Platinum single-atom and cluster catalysis of the hydrogen evolution reaction. Nat Commun 2016;7:1–9.
[68] Markovića NM, Sarraf ST, Gasteiger HA, Ross PN. Hydrogen electrochemistry on platinum low-index single-crystal surfaces in alkaline solution. J Chem Soc Faraday Trans 1996;92:3719–25.
[69] Chen Z, Lu J, Ai Y, Ji Y, Adschiri T, Wan L. Ruthenium/graphene-like layered carbon composite as an efficient hydrogen evolution reaction electrocatalyst. ACS Appl Mater Interfaces 2016;8:35132–7.
[70] Sun SW, Wang GF, Zhou Y, Wang FB, Xia XH. High-performance Ru@ C_4N electrocatalyst for hydrogen evolution reaction in both acidic and alkaline solutions. ACS Appl Mater Interfaces 2019;11:19176–82.

[71] Yao Q, Huang B, Zhang N, Sun M, Shao Q, Huang X. Channel rich RuCu nanosheets for pH universal overall water splitting electrocatalysis. Angew Chem 2019;131:14121–6.
[72] Wang Y, Sun Q, Wang Z, Xiao W, Fu Y, Ma T, Wu Z, Wang L. In situ phase-reconfiguration to synthesize Ru, B co-doped nickel phosphide for energy-efficient hydrogen generation in alkaline electrolytes. J Mater Chem 2022;10:16236–42.
[73] Wang Z, Wang Y, Xiao W, Wang X, Fu Y, Xu G, Li Z, Wu Z, Wang L. Ru, B Co-doped hollow structured iron phosphide as highly efficient electrocatalyst toward hydrogen generation in wide pH range. J Mater Chem 2022;10:15155–60.
[74] Gao Y, Zheng D, Li Q, Xiao W, Ma T, Fu Y, Wu Z, Wang L. 3D $Co_3O_4RuO_2$ hollow spheres with abundant interfaces as advanced trifunctional electrocatalyst for water splitting and flexible Zn–air battery. Adv Funct Mater 2022:2203206.
[75] Yu W, Chen Z, Xiao W, Chai Y, Dong B, Wu Z, Wang L. Phosphorus doped two-dimensional $CoFe_2O_4$ nanobelts decorated with Ru nanoclusters and Co–Fe hydroxide as efficient electrocatalysts toward hydrogen generation. Inorg Chem Front 2022;9:1847–55.
[76] Engstrom JR, Tsai W, Weinberg WH. The chemisorption of hydrogen on the (111) and (110) (1× 2) surfaces of iridium and platinum. J Chem Phys 1987;87:3104–19.
[77] Mahmood J, Anjum MA, Shin SH, Ahmad I, Noh HJ, Kim SJ, Jeong HY, Lee JS, Baek JB. Encapsulating iridium nanoparticles inside a 3D cage like organic network as an efficient and durable catalyst for the hydrogen evolution reaction. Adv Mater 2018;30:1805606.
[78] Guo X, Wan X, Liu Q, Li Y, Li W, Shui J. Phosphated IrMo bimetallic cluster for efficient hydrogen evolution reaction. eScience 2022;2:304–10.
[79] Bhowmik T, Kundu MK, Barman S. Palladium nanoparticle–graphitic carbon nitride porous synergistic catalyst for hydrogen evolution/oxidation reactions over a broad range of pH and correlation of its catalytic activity with measured hydrogen binding energy. ACS Catal 2016;6:1929–41.
[80] Hinnemann B, Moses PG, Bonde J, Jørgensen KP, Nielsen JH, Horch S, Chorkendorff I, Nørskov JK. Biomimetic hydrogen evolution: MoS_2 nanoparticles as catalyst for hydrogen evolution. J Am Chem Soc 2005;127:5308–9.
[81] Jaramillo TF, Jørgensen KP, Bonde J, Nielsen JH, Horch S, Chorkendorff I. Identification of active edge sites for electrochemical H_2 evolution from MoS_2 nanocatalysts. Science 2007;317:100–2.
[82] Cheng Y, Song H, Wu H, Zhang P, Tang Z, Lu S. Defects Enhance the electrocatalytic hydrogen evolution properties of MoS_2 based materials. Chem Asian J 2020;15:3123–34.
[83] Sharma U, Karazhanov S, Alonso-Vante N, Das S. Metallic-phase of MoS_2 as potential electro-catalyst for hydrogen production via water splitting: a brief review. Curr Opin Electrochem 2022;35:101067.
[84] Yue X, Yang J, Li W, Jing Y, Dong L, Zhang Y, Li X. Electron irradiation induces the conversion from 2H-WSe_2 to 1T-WSe_2 and promotes the performance of electrocatalytic hydrogen evolution. ACS Sustainable Chem Eng 2022;10:2420–8.
[85] Miao R, Dutta B, Sahoo S, He J, Zhong W, Cetegen SA, Jiang T, Alpay SP, Suib SL. Mesoporous iron sulfide for highly efficient electrocatalytic hydrogen evolution. J Am Chem Soc 2017;139:13604–7.
[86] Jiang N, Tang Q, Sheng M, You B, Jiang DE, Sun Y. Nickel sulfides for electrocatalytic hydrogen evolution under alkaline conditions: a case study of crystalline NiS, NiS_2, and Ni_3S_2 nanoparticles. Catal Sci Technol 2016;6:1077–84.
[87] Hota P, Bose S, Dinda D, Das P, Ghorai UK, Bag S, Mondal S, Saha SK. Nickel-doped silver sulfide: an efficient air-stable electrocatalyst for hydrogen evolution from neutral water. ACS Omega 2018;3:17070–6.
[88] Long X, Li G, Wang Z, Zhu H, Zhang T, Xiao S, Guo W, Yang S. Metallic iron–nickel sulfide ultrathin nanosheets as a highly active electrocatalyst for hydrogen evolution reaction in acidic media. J Am Chem Soc 2015;137:11900–3.
[89] Hota P, Kapuria A, Bose S, Maiti DK, Saha SK. The role of lone-pair electrons on electrocatalytic activity of copper antimony sulfide nanostructures. Mater Chem Phys 2022;291:126676.
[90] Zahra R, Pervaiz E, Yang M, Rabi O, Saleem Z, Ali M, Farrukh S. A review on nickel cobalt sulphide and their hybrids: earth abundant, pH stable electro-catalyst for hydrogen evolution reaction. Int J Hydrogen Energy 2020;45:24518–43.
[91] Li Q, Yan W, Liu Y, Du H, Wang Z, Hao X, Guan G. One-step electrodeposition of cauliflower-like $Co_zNi_yS_x$@ polypyrrole electrocatalysts on carbon fiber paper for hydrogen evolution reaction. Int J Hydrogen Energy 2019;44:12931–40.
[92] Sheebha I, Maheskumar V, Sebastian A, Vidhya B, Sakunthala A. Enhanced hydrogen evolution by rGO decorated copper nickel tin sulphide (CNTS-rGO) in acidic medium by water splitting. Int J Hydrogen Energy 2022;47:25583–94.
[93] Zhang H, Yang X, Zhang H, Ma J, Huang Z, Li J, Wang Y. Transition metal carbides as hydrogen evolution reduction electrocatalysts: synthetic methods and optimization strategies. Chem Eur J 2021;27:5074–90.
[94] Wang T, Cao X, Jiao L. Ni_2P/NiMoP heterostructure as a bifunctional electrocatalyst for energy-saving hydrogen production. eScience 2021;1:69–74.
[95] Shi D, Wu L, Chen Q, Jin D, Chen M, Shan Q, Wang D. Interface engineering of $Ni_{0.85}Se/Ni_3S_2$ nanostructure for highly enhanced hydrogen evolution in alkaline solution. Int J Hydrogen Energy 2022;47:305–13.
[96] Jiang W, Jiang Y, Wang J, Wu Y, Zhou S, Liu B, Li H, Zhou T, Liu C, Che G. Metal-organic frameworks derived N, S, O-doped carbon sheets coated CoP/Co_3S_4 hybrids for enhanced electrocatalytic hydrogen evolution reaction. Int J Hydrogen Energy 2022;47:28894–903.
[97] Zuo P, Liu Y, Liu X, Jiao W, Wang RN. P-codoped molybdenum carbide nanoparticles loaded into N,P-codoped graphene for the enhanced electrocatalytic hydrogen evolution. Int J Hydrogen Energy 2022;47:29730–40.
[98] Li Z, Wang W, Qian Q, Zhu Y, Feng Y, Zhang Y, Zhang H, Cheng M, Zhang G. Magic hybrid structure as multifunctional electrocatalyst surpassing benchmark Pt/C enables practical hydrazine fuel cell integrated with energy-saving H_2 production. eScience 2022;2:416–27.
[99] Balaji D, Madhavan J, AlSalhi MS, Aljaafreh MJ, Prasad S, Show PL. Carbon supported Ni_3N/Ni heterostructure for hydrogen evolution reaction in both acid and alkaline media. Int J Hydrogen Energy 2021;46:30739–49.
[100] Li KN, Yang CL, Wang MS, Ma XG, Wang LZ. Extraction of H_2 from H_2O molecule using a small Al_6Si cluster. Int J Hydrogen Energy 2016;41:17858–63.
[101] Xie WL, Zhang ZH, Yang CL, Wang MS, Ma XG. Hydrogen generation from water molecule with Pt_7 clusters. Int J Hydrogen Energy 2017;42:4032–9.
[102] Li KN, Yang CL, Han YX, Wang MS, Ma XG, Wang LZ. Generating H_2 from a H_2O molecule by catalysis using a small Al_6Cu cluster. Energy 2016;106:131–6.
[103] Xie WL, Zhang ZH, Yang CL, Wang MS, Ma XG. Pt_4 cluster catalyzes H_2 generation from an H_2O molecule. Chem Phys Lett 2019;725:97–101.
[104] Jaramillo TF, Bonde J, Zhang J, Ooi BL, Andersson K, Ulstrup J, Chorkendorff I. Hydrogen evolution on supported incomplete cubane-type $[Mo_3S_4]^{4+}$ electrocatalysts. J Phys Chem C 2008;112:17492–8.

[105] Kibsgaard J, Jaramillo TF, Besenbacher F. Building an appropriate active-site motif into a hydrogen-evolution catalyst with thiomolybdate $[Mo_3S_{13}]^{2-}$ clusters. Nat Chem 2014;6:248–53.
[106] Ito Y, Cong W, Fujita T, Tang Z, Chen M. High catalytic activity of nitrogen and sulfur co-doped nanoporous graphene in the hydrogen evolution reaction. Angew Chem 2015;127:2159–64.
[107] Narwade SS, Mali SM, Sathe BR. Amine-functionalized multi-walled carbon nanotubes (EDA-MWCNTs) for electrochemical water splitting reactions. New J Chem 2021;45:3932–9.
[108] Zheng Y, Jiao Y, Zhu Y, Li LH, Han Y, Chen Y, Du A, Jaroniec M, Qiao SZ. Hydrogen evolution by a metal-free electrocatalyst. Nat Commun 2014;5:1–8.
[109] Pradhan A, Manna RN. Surface-modified covalent organic polymer for metal-free electrocatalytic hydrogen evolution reaction. ACS Appl Poly Mater 2021;3:1376–84.
[110] Kori DK, Jadhav RG, Dhruv L, Das AK. A platinum nanoparticle doped self-assembled peptide bolaamphiphile hydrogel as an efficient electrocatalyst for the hydrogen evolution reaction. Nanoscale Adv 2021;3:6678–88.
[111] Mahmood J, Li F, Jung SM, Okyay MS, Ahmad I, Kim SJ, Park N, Jeong HY, Baek JB. An efficient and pH-universal ruthenium-based catalyst for the hydrogen evolution reaction. Nat Nanotechnol 2017;12:441–6.
[112] Kweon DH, Okyay MS, Kim SJ, Jeon JP, Noh HJ, Park N, Mahmood J, Baek JB. Ruthenium anchored on carbon nanotube electrocatalyst for hydrogen production with enhanced Faradaic efficiency. Nat Commun 2020;11:1–10.
[113] Yin Y, Zhang Y, Gao T, Yao T, Zhang X, Han J, Wang X, Zhang Z, Xu P, Zhang P, Cao X. Synergistic phase and disorder engineering in 1T-$MoSe_2$ nanosheets for enhanced hydrogen evolution reaction. Adv Mater 2017;29:1700311.
[114] Jin Y, Wang H, Li J, Yue X, Han Y, Shen PK, Cui Y. Porous MoO_2 nanosheets as non-noble bifunctional electrocatalysts for overall water splitting. Adv Mater 2016;28:3785–90.
[115] Kuang M, Han P, Wang Q, Li J, Zheng G. CuCo hybrid oxides as bifunctional electrocatalyst for efficient water splitting. Adv Funct Mater 2016;26:8555–61.
[116] Zhu Y, Chen G, Xu X, Yang G, Liu M, Shao Z. Enhancing electrocatalytic activity for hydrogen evolution by strongly coupled molybdenum nitride@ nitrogen-doped carbon porous nano-octahedrons. ACS Catal 2017;7:3540–7.
[117] Zhang Y, Ouyang B, Xu J, Chen S, Rawat RS, Fan HJ. 3D porous hierarchical nickel–molybdenum nitrides synthesized by RF plasma as highly active and stable hydrogen-evolution-reaction electrocatalysts. Adv Energy Mater 2016;6:1600221.
[118] Yin Y, Han J, Zhang Y, Zhang X, Xu P, Yuan Q, Samad L, Wang X, Wang Y, Zhang Z, Zhang P. Contributions of phase, sulfur vacancies, and edges to the hydrogen evolution reaction catalytic activity of porous molybdenum disulfide nanosheets. J Am Chem Soc 2016;138:7965–72.
[119] Wang H, Li XB, Gao L, Wu HL, Yang J, Cai L, Ma TB, Tung CH, Wu LZ, Yu G. Three-dimensional graphene networks with abundant sharp edge sites for efficient electrocatalytic hydrogen evolution. Angew Chem 2018;130:198–203.
[120] Tan Y, Luo M, Liu P, Cheng C, Han J, Watanabe K, Chen M. Three-dimensional nanoporous $Co_9S_4P_4$ pentlandite as a bifunctional electrocatalyst for overall neutral water splitting. ACS Appl Mater Interfaces 2019;11:3880–8.
[121] Sarno M, Ponticorvo E, Scarpa D. Active and stable graphene supporting trimetallic alloy-based electrocatalyst for hydrogen evolution by seawater splitting. Electrochem Commun 2020;111:106647.